Linking strike directions to invariant TE and TM impedances of the magnetotelluric impedance tensor

Rocio Fabiola Arellano-Castro (rarellan@cicese.edu.mx)
CICESE https://orcid.org/0000-0003-4413-8653
Enrique Gómez-Treviño
CICESE: Centro de Investigacion Cientifica y de Educacion Superior de Ensenada

Full paper

Keywords: Strike direction, invariants TE and TM, Phase tensor

Posted Date: April 26th, 2021

DOI: https://doi.org/10.21203/rs.3.rs-444935/v1

Linking strike directions to invariant TE and TM impedances of the magnetotelluric impedance tensor

Rocío F. Arellano-Castro* and Enrique Gómez-Treviño*
*CICESE, División de Ciencias de la Tierra, Ensenada, Baja California, México. 22860

ABSTRACT

The traditional transverse electric (TE) and transverse magnetic (TM) impedances of the magnetotelluric tensor can be decoupled from the strike direction with significant implications when dealing with galvanic distortions. Distortion-free impedances are obtainable combining a quadratic equation with the phase tensor. In the terminology of Groom-Bailey, the quadratic equation provides amplitudes and phases that are immune to twist and the phase tensor provides phases immune to both, twist and shear. On the other hand, distortion-free strike directions can be obtained using Bahr's approach or the formula provided by the phase tensor. In principle, this is all that is needed to proceed to a two-dimensional (2D) interpretation. However, the resulting impedances are strike-ignorant because they are invariant under rotation and, if they are to be related to a geological strike they must be linked to a particular direction. This is an extra ambiguity beside the classical of 90 degrees which must be resolved independently. In this work we use the distortion model of Groom-Bailey to resolve the ambiguity by bringing back the coupling between impedances and strike in the presence of galvanic distortions. Considering that most quantities are already known, fitting the responses of the model to the data requires minimizations only over the single variable of twist, instead of the original approach of having to minimize not only twist, shear and strike, but also the impedances themselves. Our approach is a hybrid between existing numerical and analytical

approaches that reduces the problem to a binary decision. The fusion of the two approaches is illustrated using synthetic and field data.

Keywords: Strike direction, invariants TE and TM, Phase tensor.

*Correspondence: rarellan@cicese.edu.mx. Departamento de Geofísica Aplicada, División de Ciencias de la Tierra, CICESE, 22860 Ensenada, Baja California, México.

INTRODUCTION

The basic unit of the magnetotelluric (MT) method of geophysical prospecting is a 2x2 complex tensor per frequency in a given range of frequencies. The measurements are usually taken in a coordinate system that is not the one ultimately used in the final interpretation. In general, the matter of going from one system to the other is far from trivial as explained by Groom and Bahr (1992) in their classical tutorial paper. When it is assumed that the target is a two-dimensional (2D) structure, one of the axes must be parallel to the strike of the structure. It used to be common practice to find the appropriate angle simply by applying the traditional rotation matrix. However, this may lead to erroneous results when the data are polluted by what is known as galvanic distortions (e.g. Bahr, 1988). “Rotate at your peril” is the subtitle of a paper by Jones and Groom (1993) where the matter is discussed at length. They use the distortion model of Groom and Bailey (1989) to correct for three-dimensional (3D) effects of otherwise 2D undistorted data. The approach consists of fitting the data with the response of the model, which includes as unknowns the angle of rotation and two distortion parameters, along with the undistorted data which consist of an anti-diagonal 2x2 complex tensor. The algorithm STRIKE based on the extensions made by McNeice and Jones (2001) is the standard for 2D applications. Jones (2012) enumerates four advantages of the approach over other methods. Here we use a fifth one. It is the rather obvious fact that the undistorted impedances are linked to a strike direction. This coupling is important because if the impedances are to be related to a geological strike they must be linked to a particular direction. This fifth advantage of the distortion model is a feature missing in other methods for estimating the impedances as discussed in the following paragraphs.

The link between strikes and impedances comes naturally. For instance, the classical approach of Swift (1967) minimizes the size of the diagonal elements of the impedance tensor to find the optimum strike. Then, the measured tensor is rotated to obtain the new elements in the rotated coordinates. Swift's approach was developed before the community recognized and tried to overcome the effects of the galvanic distortions. Bahr (1988) realized that a strike direction immune to galvanic distortions could be obtained by imposing the same phase on the columns of the impedance tensor. He developed an analytic formula for strike that is immune to galvanic distortions. However, even if one has an undistorted strike and use it to rotate a distorted impedance tensor, the result can't be but a distorted tensor. In contrast, in the Groom-Bailey approach the fitting process optimizes simultaneously the strike direction and the undistorted data, since they are coupled from the beginning. One of the outcomes is that there is no need for further rotations.

Other methods don't need the strike angle to estimate the undistorted impedances. In this case the impedances are decoupled from the strike. This is possible by the use of invariants under rotation of coordinates. Of the stockpile of invariants of the impedance tensor that have been proposed in the literature some have a special property when applied in 2D: they reduce to the traditional *TE* and *TM* impedances. One pair of these invariants, $\Phi_{\max}$ and $\Phi_{\min}$, is derived from the phase tensor of Caldwell et.al, (2004). Another pair, represented as complex resistivities $\varrho_{\pm}$, is derived from a quadratic equation (Gómez-Treviño et. al, 2014a). We use this last pair in this work. The idea is to restore the strike direction lost when formulating the quadratic equation for the invariants. The issue does not exist if strikes and impedances are treated independently as in Muñiz et

al. (2017). However, when inverting the data we need to link a strike angle to either ϱ_+ or ϱ_-. This is of course impossible on the grounds of how they are computed. The resistivities are invariant under rotation so they have no specific angle. On the other hand, whether the strike is computed using Bahr's formula or the phase tensor it is decoupled from the undistorted impedances. All things considered, the price for going analytical is further uncertainty beyond the classical 90 degrees ambiguity. There is no major difficulty when the strike is small, or when the modes are easily identifiable as in a recent application in a marine environment (Montiel-Álvarez et al., 2020). However, if this is not the case the situation can become helpless. Interpreting the well-known BC87 data set, much to our dismay we had to recur to the algorithm STRIKE simply to identify the modes (Gómez-Treviño et al., 2018), although the rest of the analysis was based on the $\varrho_\pm$ formulae. To simply identify the modes there are other alternatively. The logical thing to do would be to insert back the $\varrho_\pm$ analysis into the original Groom-Bailey distortion model. This would come naturally since the resistivities $\varrho_\pm$ were developed precisely as solutions of this model. In this work we explore this alternative using several new developments on the subject.

METODOLOGY

The Groom-Bailey decomposition

Let us begin by assuming that for a given frequency or period we have a complex impedance tensor $\boldsymbol{Z}$ given as

$$\boldsymbol{Z} = \begin{pmatrix} Z_{xx} & Z_{xy} \\ Z_{yx} & Z_{yy} \end{pmatrix}. \tag{1}$$

The impedance tensor is the elementary unit of the MT method but to make it represent the real Earth some modifications are needed. Small, near surface heterogeneities that are of no interest can severely distort the elements of the tensor. These effects can be modeled using a dimensionless and frequency independent 2x2 real matrix $\boldsymbol{C}$ (e.g., Bahr (1988). The distorted or measured impedance tensor would be $\boldsymbol{Z}_m = \boldsymbol{CZ}$. The elements of $\boldsymbol{C}$ must be determined or avoided in order to have distortion-free data. The Groom and Bailey (1989) decomposition opts for determining them by first separating those that are determinable from those that are not. The decomposition is represented as

$$\boldsymbol{Z}_m = \boldsymbol{RTSAZ_2R}^T. \qquad (2)$$

The different factors are shown explicitly in Table 1. It is assumed that the undistorted impedances $\boldsymbol{Z_2}$ are 2D. The rotation matrix $\boldsymbol{R}$ and its transpose $\boldsymbol{R}^T$ depend only on one parameter, the strike angle θ. The twist tensor $\boldsymbol{T}$ depends also on one parameter t, as does the shear tensor $\boldsymbol{S}$ with its variable e. The tensor $\boldsymbol{A}$ contains two parameters a and b that are not considered unknowns. They are absorbed as real scaling factors by the undistorted impedances. They account for the well-known static effect on the measured electric field. The full realization that these factors are not determinable from the impedances alone came with the work of Bostick (1984; 1986). The decomposition perfectly acknowledges this fact. Also, something that is not often mentioned is that the factors are applied in the coordinates of the undistorted impedances, and not where the measurements were made and where the statics physically originates. However, this is how it should be since the undistorted impedances are the ones that are ultimately

interpreted. If data are available for several nearby sites the factors can be estimated using existing inverse routines in anti-Occam mode (Gómez-Treviño et al., 2014b; 2018). Nevertheless, this can be done only after the scaled impedances are obtained, and they are derived by fitting the distortion model on the right hand side of equation 2 to the measured impedances on the left hand side of the same equation. The problem consists of finding the impedances as well as the distortion parameters twist and shear and also the strike direction. The solution is obtained by minimizing the fit to the data using the objective function

$$\chi^2 = \frac{1}{4n_T}\sum_{i=1}^{n_T}\left\{\sum_{j=1}^{2}\sum_{k=1}^{2}\frac{\left|Z_{mjk}(T_i) - Z_{cjk}(T_i)\right|^2}{\sigma_{jk}^2(T_i)}\right\}, \qquad (3)$$

where n_T is the number of periods T_i, Z_{mjk} is the measured impedance and σ_{jk}^2 is the corresponding variance, and Z_{cjk} is the computed impedance from the distortion model. The algorithm STRIKE of McNeice and Jones (2001) uses quadratic programming and is the standard for the community of interpreters.

Groom-Bailey Decomposition

$$\boldsymbol{Z}_m = \boldsymbol{RTSAZ_2R}^T.$$

Rotation

$$\boldsymbol{R} = \begin{pmatrix} cos\theta & sin\theta \\ -sin\theta & cos\theta \end{pmatrix}$$

Twist

$$\boldsymbol{T} = \frac{1}{\sqrt{1+t^2}}\begin{pmatrix} 1 & -t \\ t & 1 \end{pmatrix}$$

Shear

$$\boldsymbol{S} = \frac{1}{\sqrt{1+e^2}}\begin{pmatrix} 1 & e \\ e & 1 \end{pmatrix}$$

Scaling

$$\boldsymbol{A} = \begin{pmatrix} a & 0 \\ 0 & b \end{pmatrix}$$

2D impedances

$$\boldsymbol{AZ}_2 = \begin{pmatrix} 0 & aZ_{2xy} \\ bZ_{2yx} & 0 \end{pmatrix}$$

Table 1. The measured impedance tensor is represented as $\boldsymbol{Z}_m$. The rest of the tensors are defined in terms of one or more parameters which are to be determined in the fitting process.

The quadratic equation

The Groom-Bailey factorization or decomposition given by equation 2 has some peculiar properties that allow the direct computation of almost distortion-free impedances. This can be done using the quadratic equation proposed by Gómez-Treviño et al., (2014a). Defining complex resistivities $\varrho_{ij} = (1/\omega\mu_0)Z_{ij}^2$, where ω stands for angular frequency and μ_0 for the magnetic permeability of free space, the distortion-free resistivities associated with $\boldsymbol{Z_2}$ can be computed as $Z_\pm = \sqrt{\omega\mu_0\varrho_\pm}$ from

$$\varrho_\pm = \varrho_{sm} \pm \sqrt{\varrho_{sm}^2 + \varrho_{sm}\varrho_{pm}\varepsilon^{-2}}, \qquad (4)$$

where

$$\varrho_{sm} = \frac{1}{2}\left(\varrho_{xxm} + \varrho_{xym} + \varrho_{yxm} + \varrho_{yym}\right), \tag{5}$$

$$\varrho_{pm} = 2\frac{\left(\varrho_{xxm}\varrho_{yym} - \varrho_{xym}\varrho_{yxm}\right)^2}{\varrho_{xxm} + \varrho_{xym} + \varrho_{yxm} + \varrho_{yym}} \tag{6}$$

and

$$\varepsilon = \left(\frac{1-e^2}{1+e^2}\right). \tag{7}$$

The factor ε^{-2} within the square root sign in equation 4 corrects for the effect of shear. The formula is immune to twist and also to the strike angle because ϱ_{sm} and ϱ_{pm} are invariant under rotation. To find the adequate factor ε^{-2} it is not necessary to recur to the distortion model; it can be calculated independently in two different ways. One is to alter the measured data with static factors and then compare the phases $\varphi_{\pm}$ of the two scenarios for all possible shear values. The phases are equal or about equal only at the adequate shear. The other way is to compare $\varphi_{\pm}$ with ϕ_{max} and ϕ_{min} from the phase tensor for all possible shear values. Both types of phases are invariant and reduce in 2D to the traditional TE and TM modes.

The other distortion-free parameter that can be obtained without having to fit the data with the distortion model is the strike angle. Bahr (1988) developed an analytic formula for the strike by noticing that the columns of the distorted 2D tensor must have the same phase. A more general formula derived from the phase tensor of Caldwell et.al, (2004) includes the recognition of 3D effects. In both cases the formulas provide strikes

period by period which in some cases are not consistent showing instability (e.g. Jones, 2012). However, it is possible to obtain stable strikes by using windows of several contiguous periods (Muñiz et al., 2017; Bravo-Osuna et al., 2021).

When fitting the distortion model to the data we obtain impedances Z_{xy} and Z_{yx} that are coupled with a strike angle. If we decide for the complementary angle in view of the classical 90 degrees ambiguity the impedances simply interchange roles and the coupling is now with the corresponding angle. This coupling between impedances and strikes is missing in the approach of using the quadratic equation and the formulas for strike. In other words, it is not possible to associate $Z_{\pm}$ with the pair (Z_{xy}, Z_{yx}) . This association is important because it is the connection between the physics and the local geology which helps to decide over the classical ambiguity. In order to make the proper association we have to return to the distortion model.

The distortion model has seven real unknowns, four from the impedances, one from the strike and two from twist and shear. Of the seven we already know five and the absolute value of one: we only need the sign of shear and the value of twist. This means that the dilemma of which mode is which can be solved by minimizing χ^2 only over one variable twice, one for negative and one for positive shear. The correct sign would fit the data better. Also, there is no need to include all the data because we are not trying to optimize neither the impedances nor the strike since they are already known. It would be sufficient to compare, for instance, only the fit to the amplitudes or to the amplitudes of a single mode because the problem is reduced to a binary decision. In the following section we present results to explain step by step how to relate strikes to invariant TE and TM impedances.

RESULTS

Linking strike angles to the TE and TM invariants requires several steps. On one side we have the quadratic equation that provides the impedances and on the other the determination of the strike. The impedances depend on the absolute value of shear and to make them distortion-free their phases are modified to fit those of the phase tensor. At this point they are ready to be placed on the distortion model. On the other side we have the strike angle which is obtained independently and can also be substituted in the rotation matrix. The only unknowns are the sign of shear and the value of twist. The hypothesis is that when optimizing for twist the plus and minus signs of shear lead to very different fits to the data. Selecting the adequate sign is the last step. The rest would consist of checking, for instance, the *xy* curves of model and data to see if they match. If they do, then the strike corresponds to the chosen invariant as the *xy* component. If they don't there is no problem, it would simply mean that the invariants must be interchanged. It is in this sense that linking strike angles to invariants is a binary decision.

The basic association: strike and impedances

We begin with a very simple case where both twist and shear are zero. The idea is to explain how the binary decision works without the interference of the two distorting parameters. We present an example using synthetic ideal data with very small random errors. We chose site 15 of the COPROD2S1 data set proposed by Varentsov (1998). The data are provided as apparent resistivities and phases for 12 periods. They are

shown in Figure 1. They represent the target that must be recovered from rotated, distorted and noisy versions of them.

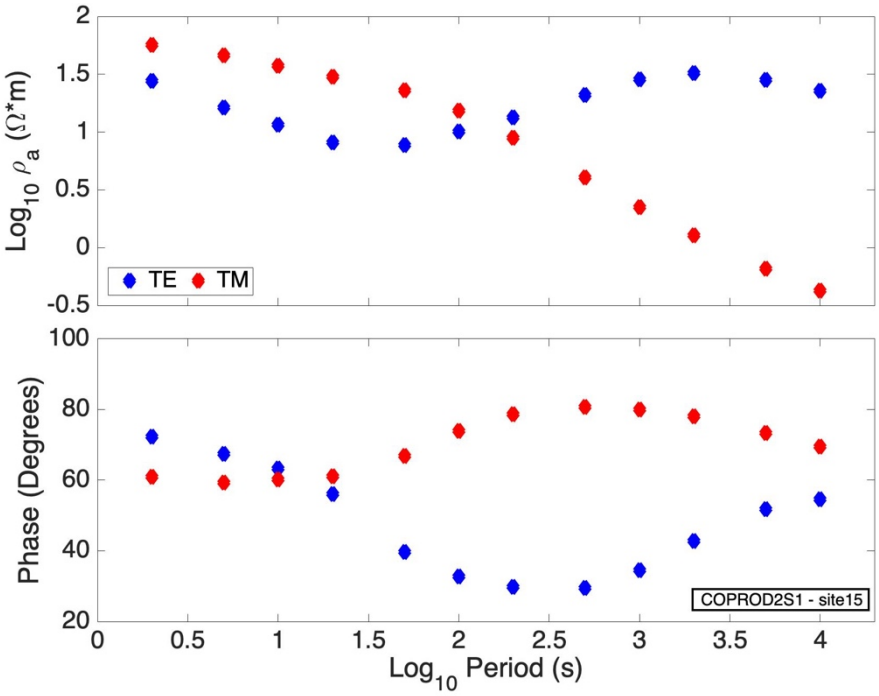

Figure 1. The original apparent resistivity and phase curves of the site 15 from the COPROD2S1 dataset. These curves are the objective of the recovery process from distorted versions of them.

Figure 2 shows the rotated version of the curves shown in Figure 1. It is assumed that the TE mode is the *xy* component. The strike is 30 degrees for the 12 periods both twist and shear are given zero values. The apparent resistivity and phase values were converted to impedances to make the rotation and to add a small random error of 0.1% of the main impedances. Then they were converted back to apparent resistivity and phase values. Notice that the main resistivities *xy* and *yx* keep some resemblance with the original unrotated resistivities. This won't happen when later on when we add galvanic distortions.

Notice also that there appears to be one component missing. What happens is that the component *yy* is on top of the component *xx* because the rotated tensor is still 2D and one of its properties is that it is symmetric. Again, this won't happen when galvanic distortions are included because they actually simulate 3D effects.

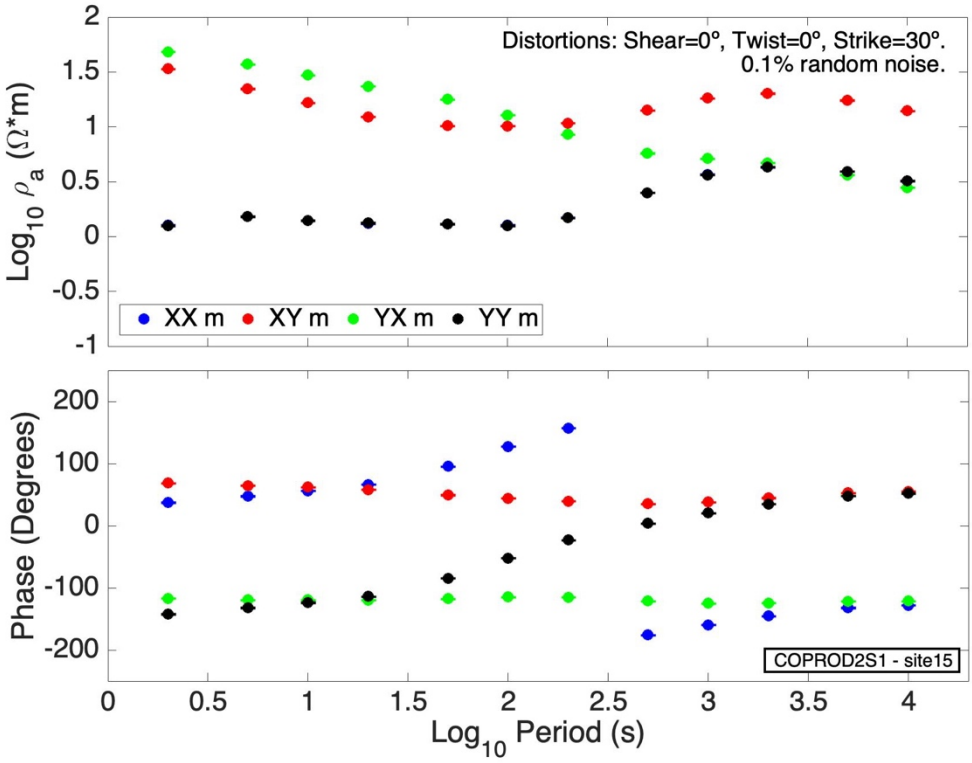

Figure 2. Distorted apparent resistivity and phase curves of site 15 from the COPROD2S1 dataset. These curves are the input for the process whose objective is the recovery of the undistorted curves of Figure 1. The distorting parameters are strike 30, twist 0 and shear 0 degrees. The random noise is 0.1 %.

The recovery of the original data of Figure 1 is shown in Figure 3. We applied equation 4 to compute $\varrho_{\pm}$. They are presented in Figure 3 as their amplitudes $\rho_{\pm}$ and phases $\varphi_{\pm}$. The recovery is excellent but it is ambiguous in the sense that we don't know which mode is TE and which is TM. Had we rotated the original data 45, 68 or -39 degrees

we cannot but obtain the same curves shown in Figure 3. This is what is meant to be invariant under rotation of coordinates. However, the strike can be determined independently within an ambiguity of 90 degrees by some other means. Let us assume for the moment that we have applied one of the available methods and that we found 30 degrees, or equivalently -60 degrees considering the classical ambiguity. Using 30 degrees in equation 2 and assuming $Z_+ = Z_{xy}$, $Z_- = Z_{yx}$ and $Z_{xx} = Z_{yy} = 0$ the result of the product is the computed response of the distortion model that can be compared with the measured impedances.

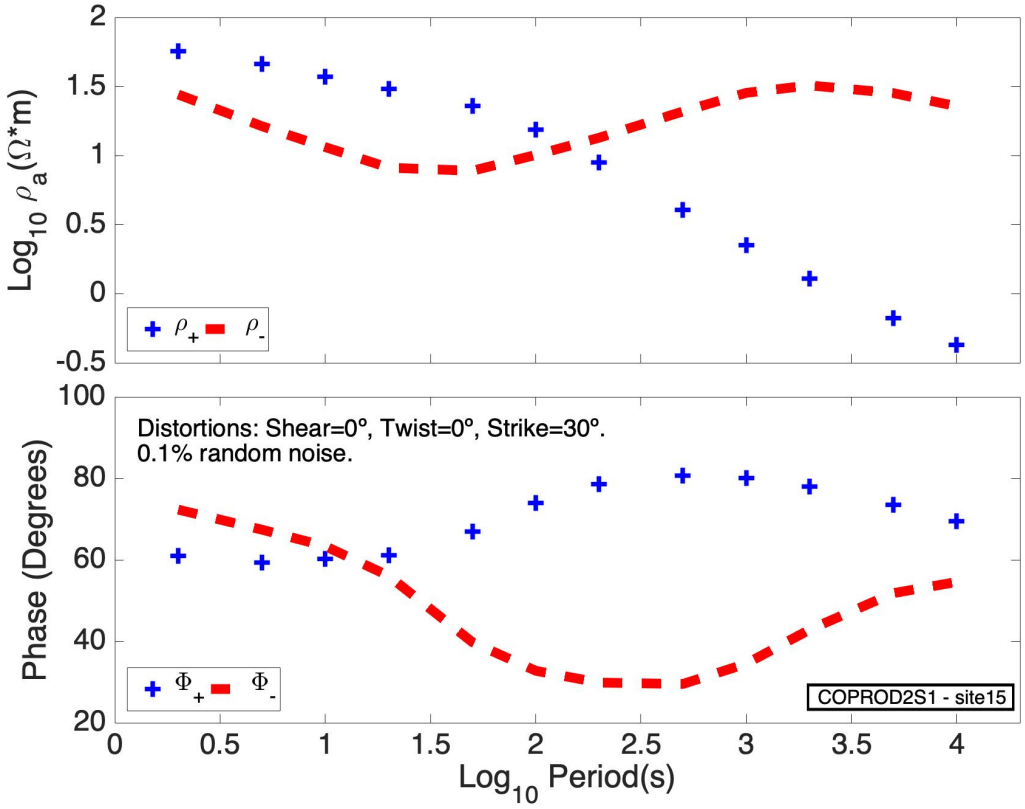

Figure 3. Recovered apparent resistivities $\rho_\pm$ and phases $\phi_\pm$ through the application of the quadratic equation. Notice that the curves are the same as the original ones. However, in this case we lose track of the strike because the quadratic equation provides invariant values under rotation.

The measured apparent resistivities are compared in Figure 4 with the corresponding values of the calculated responses. We show only the *xy* and *yx* apparent resistivities and their phases. It can be observed that the measured and computed *xy* components do not correspond at all, and the same for the *yx* components. Actually, they match each other but as opposite modes. The match is not perfect although it should be. We think this may be due to the random errors. Anyway, the important thing is that the hypothesis that a strike of 30 degrees corresponds to assuming ρ_+ as ρ_{xy} does not hold, and that we should instead assume ρ_+ as ρ_{yx} for the same strike.

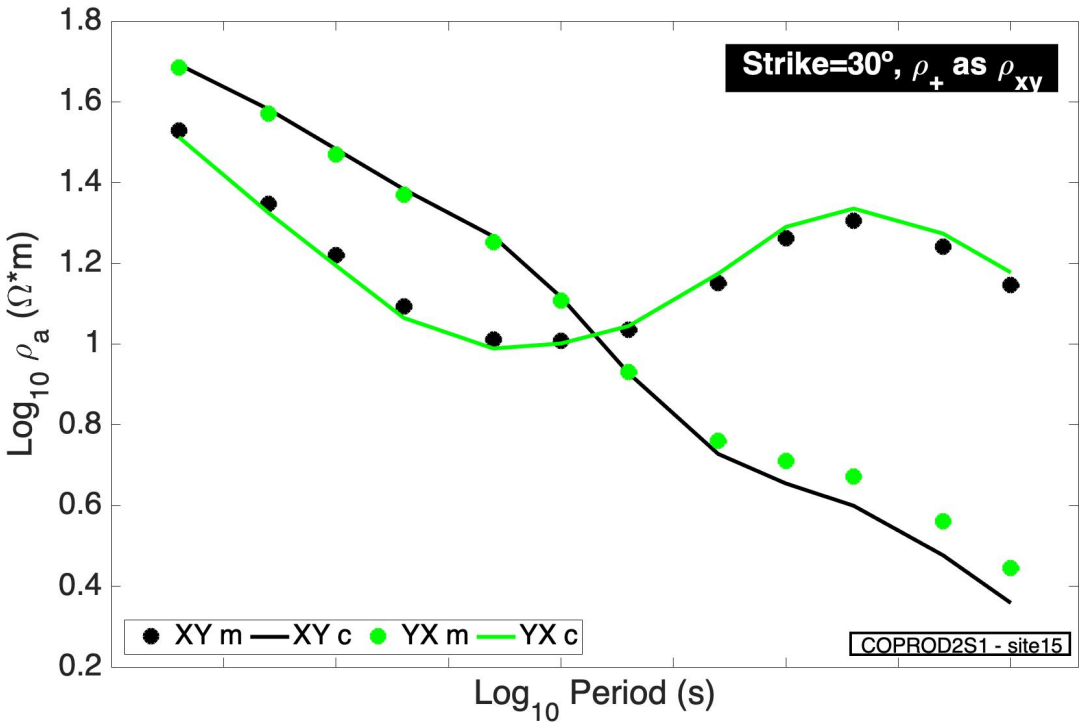

Figure 4. Comparison of the distorted data with the response of the distortion model assuming that ρ_+ is ρ_{xy} and a strike of 30 degrees. We present only the corresponding components xy and yx. It can be observed that the computed resistivities fall in the reverse sense as expected if the hypothesis was to hold. This means that we should identify a strike of 30 degrees with ρ_+ as ρ_{yx}.

It is shown in Figure 5 that assuming ρ_+ as ρ_{yx} for the strike of 30 degrees makes the measured and computed components correspond to each other. This means that when inverting the data we should interpret ρ_+ as the TM mode and ρ_- as the TE mode, provided a strike of 30 degrees has been decided from some other means. Of course, this second check to corroborate the correct association is not strictly necessary. The results shown in Figure 4 actually predict those in Figure 5. We decided to include them simply for completeness and for didactical purposes. The same goes for the next two figures that consider the complementary angle of -60 degrees.

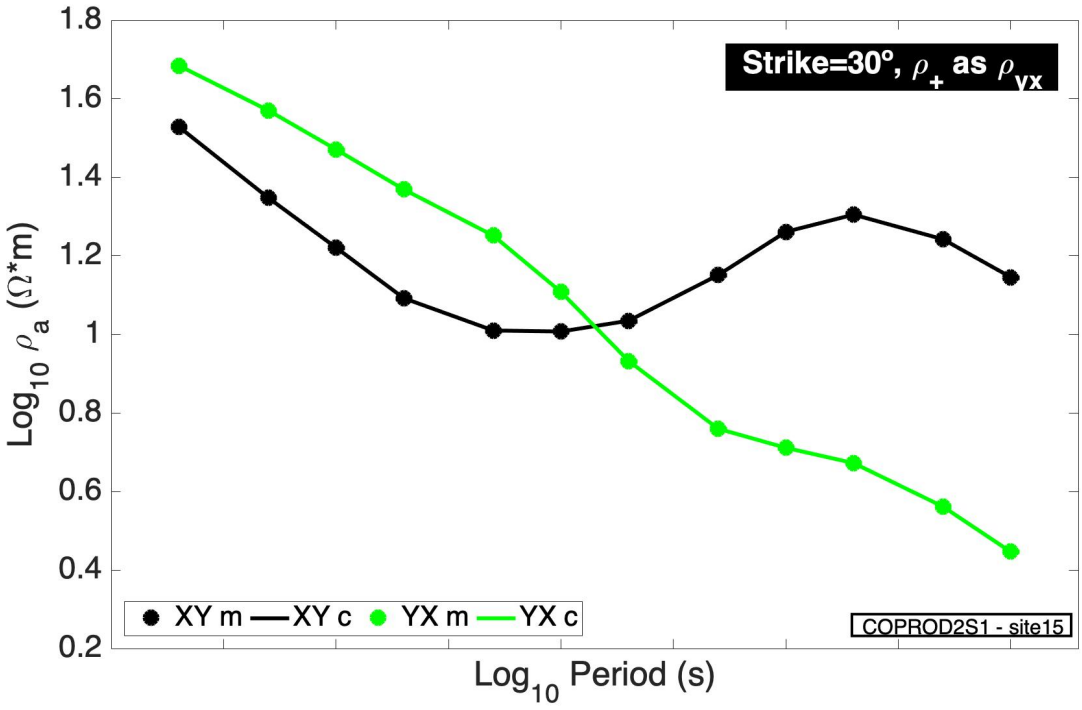

Figure 5. Comparison of the distorted data with the response of the distortion model assuming that ρ_+ is ρ_{yx} and a strike of 30 degrees. We present only the corresponding components xy and yx. It can be observed that the computed resistivities fall in the correct sense. This means that we should identify a strike of 30 degrees with ρ_+ as ρ_{yx}.

Completely compatible with Figures 4 and 5 are the results of the next two figures. Figure 6 shows the case of assuming a strike of -60 degrees and ρ_+ as ρ_{yx}. The mismatch of the components indicates that this is not the proper association. The proper association for this strike is ρ_+ as ρ_{xy} as explicitly shown in Figure 7. All four figures, from 4 to 7, provide the same information so that any of the tests can predict the other three. In general this won't be the case as discussed below.

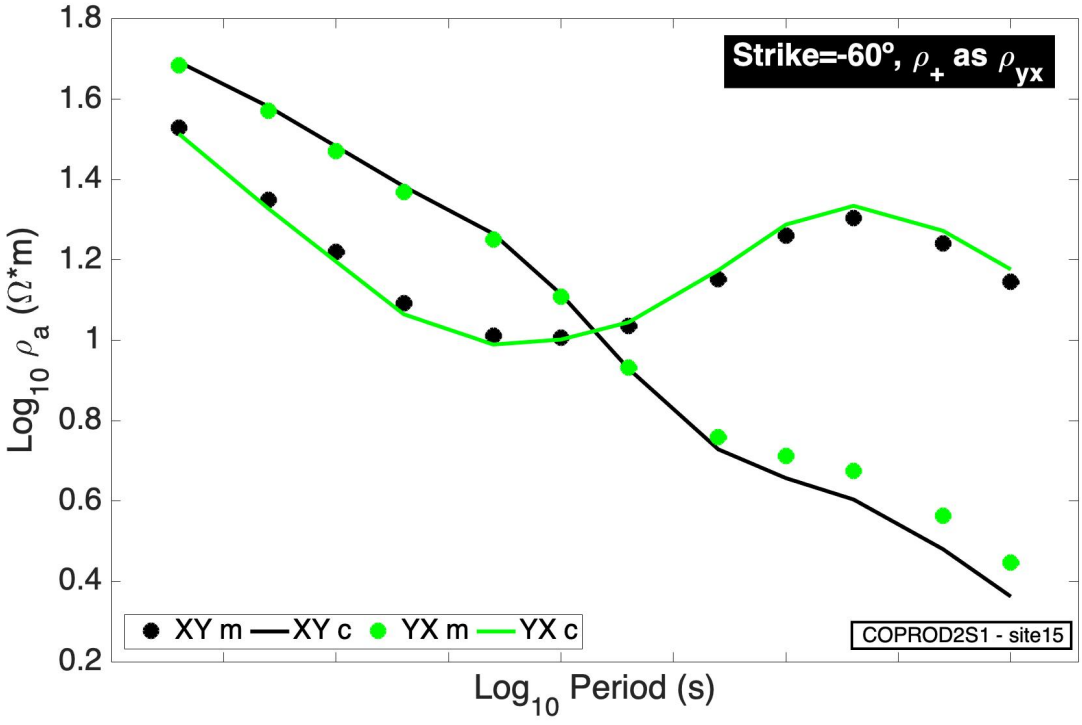

Figure 6. Comparison of the distorted data with the response of the distortion model assuming that ρ_+ is ρ_{yx} and a strike of -60 degrees. We present only the corresponding components xy and yx. It can be observed that the computed resistivities fall in the reverse sense as expected if the hypothesis was to hold. This means that we should identify a strike of -60 degrees with ρ_+ as ρ_{xy}. This is equivalent to the conclusion derived from Figure 4.

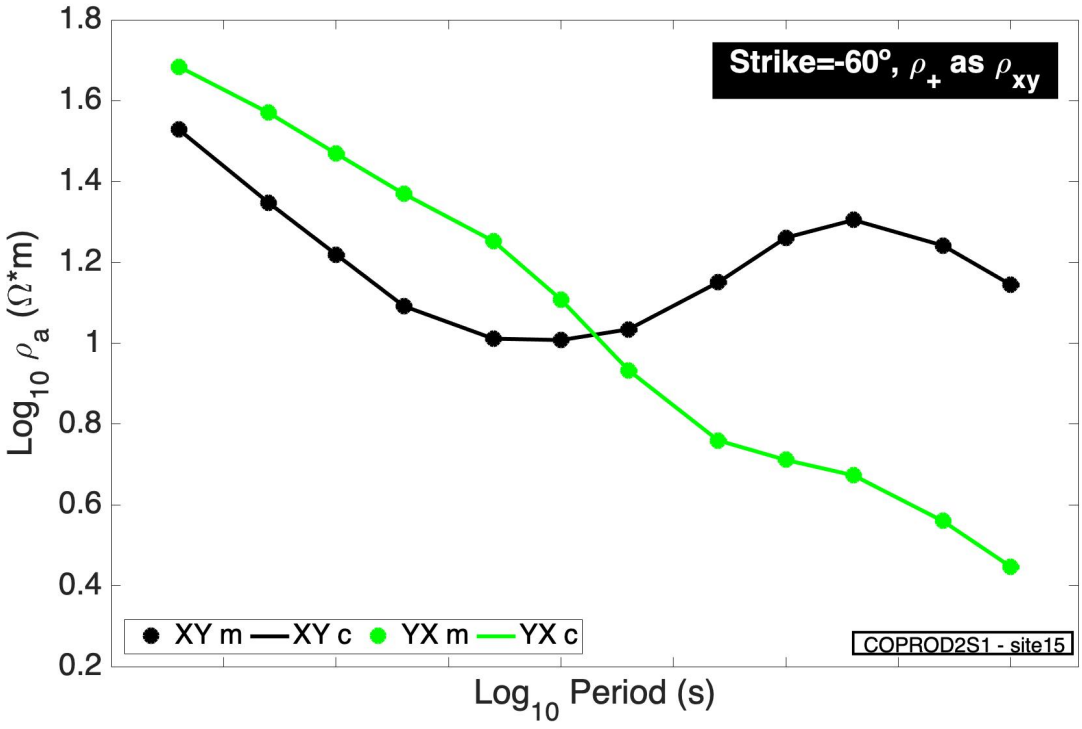

Figure 7. Comparison of the distorted data with the response of the distortion model assuming that ρ_+ is ρ_{xy} and a strike of -60 degrees. We present only the corresponding components xy and yx. It can be observed that the computed resistivities fall in the correct sense. This means that we should identify a strike of -60 degrees with ρ_+ as ρ_{xy}. This is equivalent to the conclusion derived from Figure 4.

Sign of shear and determination of twist

We now consider the case of distorted data with still very small random noise. In equation 2 the matrixes $\boldsymbol{T}$ and $\boldsymbol{S}$ are no longer identities. We use a value of twist of 20 degrees and a shear of 30 degrees. The resulting apparent resistivity and phase values are shown in Figure 8. Notice that now they show very little resemblance with the original data. Also, the resulting tensor is no longer 2D as in the previous case. This surfaces from the fact that the diagonal elements are no longer on top of each other.

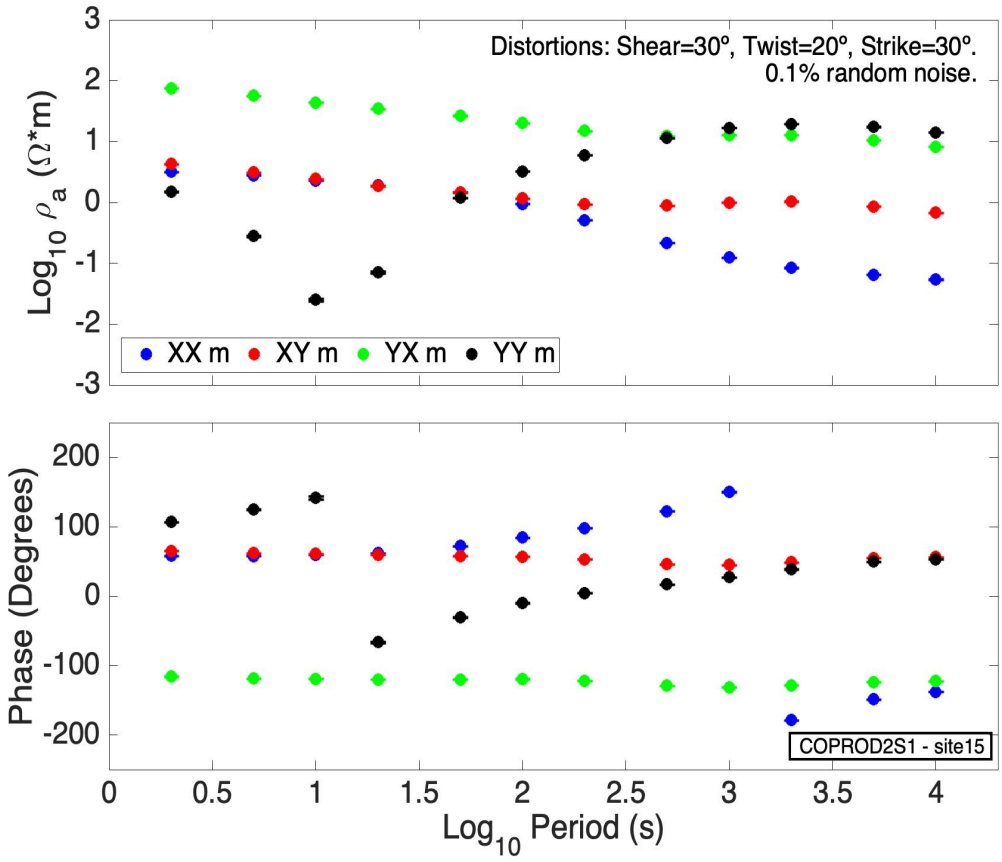

Figure 8. Distorted apparent resistivity and phase curves of site 15 from the COPROD2S1 dataset. These curves are the input of the process whose objective is the recovery of the undistorted curves of Figure1. The distorting parameters are strike 30, twist 20 and shear 30 degrees. The random noise is 0.1 %.

We assume that the absolute value of shear is known. The object of the exercise is to find out its sign and also the value of twist. Again, the impedances are computed using equation 4 which provide distortion free-values because it is being corrected for the effect of shear. Figure 9 show the penalty function χ^2 as a function of twist for the two possibilities of plus and minus signs. It can be observes that there is a large difference in the fit to the data between one sign and the other. For the positive shear the minimum is

exactly over the correct twist. It is interesting that for the negative shear the minimum also falls near the true twist of 20 degrees. However, given the large difference in the misfit there is no doubt that the sign of shear must be positive and that the twist value must be 20 degrees. The fit to the data for both positive and negative signs of shear is shown in Figure 10. We show only the *xy* and *yx* components. It can be observed that definitively the best fit is for the positive sign.

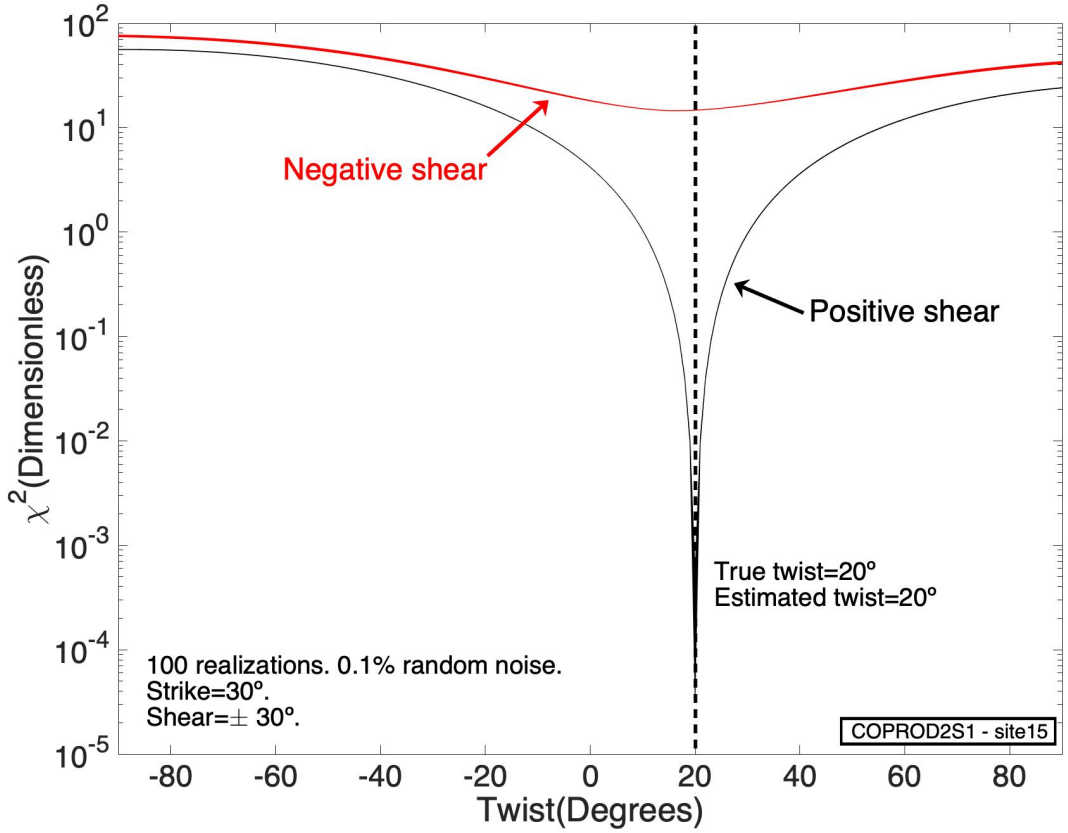

Figure 9. χ^2 objective functions for the estimation of twist assuming the two possibilities for the unknown sign of shear. It can observed that the lowest minimum corresponds to the correct positive shear.

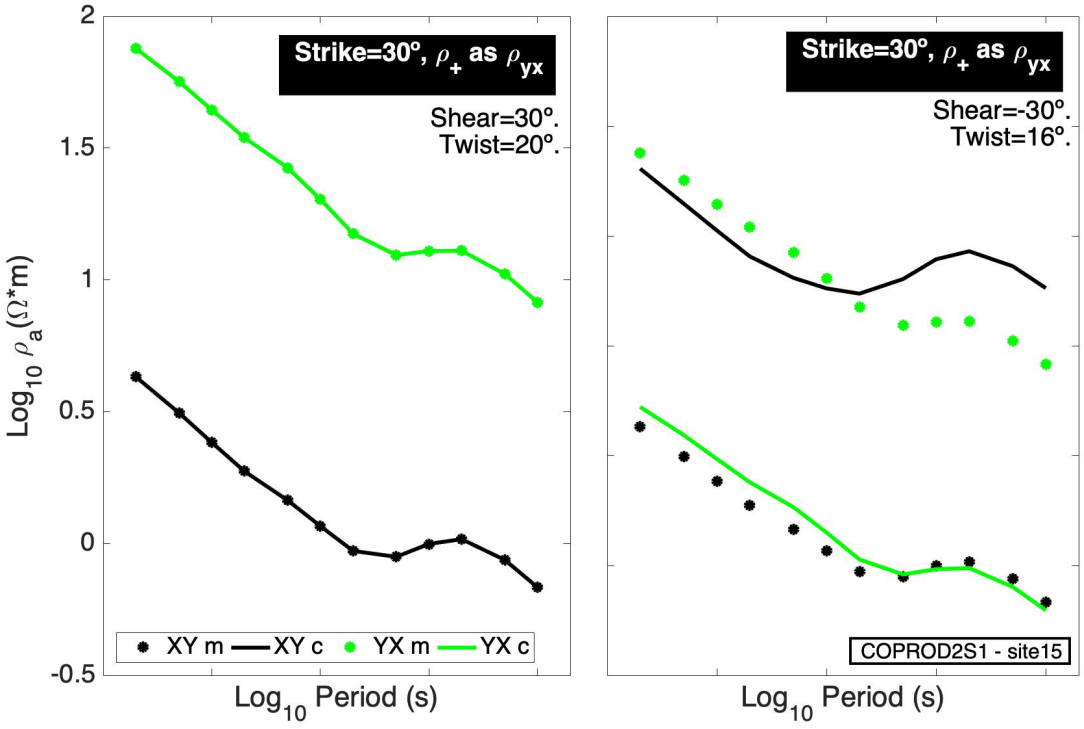

Figure 10. Comparison of the distorted data with the response of the distortion model assuming positive and negative signs for the value of shear and a twist value of 20 degrees.. We present only the corresponding components xy and yx. It can be observed that the computed resistivities fall in the correct place for the positive shear.

General case

In the previous sections we left out the estimation of some parameters in order to center around the main problem of linking strike angles to impedances. It is time to present the general case without any assumptions. The data set is the same except that the random errors were increased from 0.1 to 5 % to make it more realistic. Figure 11 shows the estimation of the strike using a reframed versión of the phase tensor (Bravo-Osuna et al., 2021). The approach allows optimization over windows of several periods. In this case the estimate is based on using all the 12 periods. The penalty function

depends on the strike and in 2D is the norm of the offdiagonal elements of the phase tensor. The estimate using 100 realizations is within less than a degree from the true value of 30 degrees.

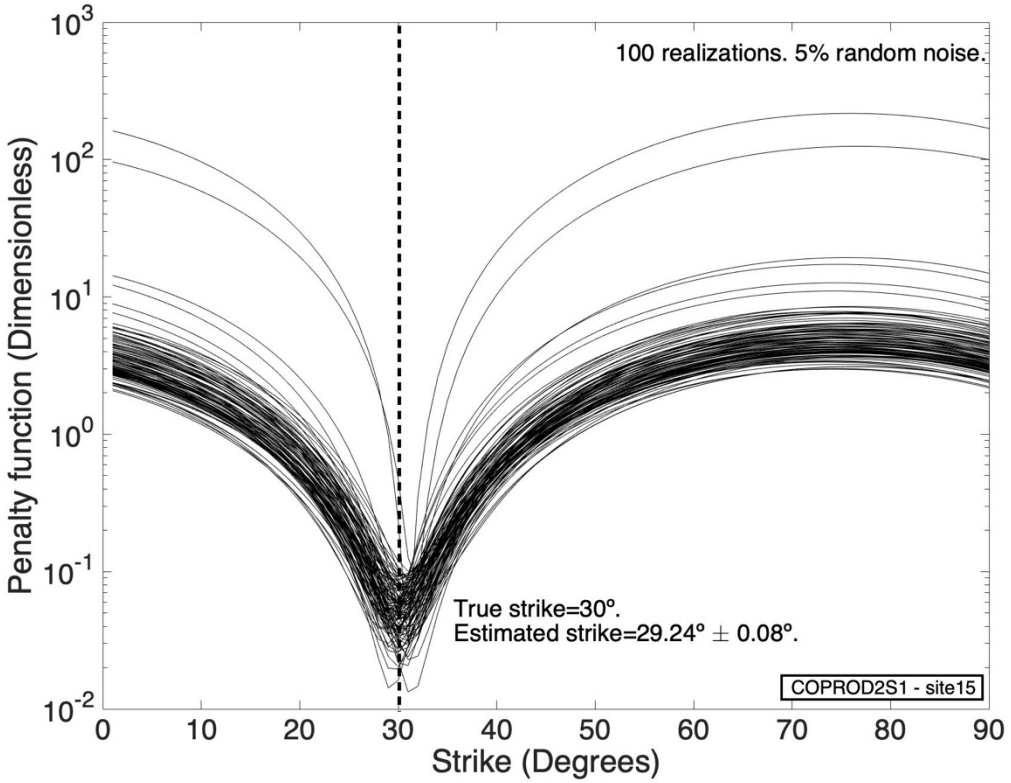

Figure 11. Estimation of strike using a reframed version of the phase tensor for a window of all 12 periods.

We now come to the estimation of the absolute value of shear. This is also obtained through optimization. Equation 4 provides phases $\varphi_{\pm}$ that depend on the square of shear. On the other hand, the phases Φ_{max} and Φ_{min} from the phase tensor don't depend on shear and reduce in 2D to the phases of the TE and TM modes. The penalty function in this case is the norm of the difference between the phases of the two approaches. The penalty function depends on the absolute value of shear and in principle it should be zero at the appropriate shear. More details can be found in Muñiz et al., (2017). Again, the estimate is very close to the true value of 30 degrees as shown in Figure 12.

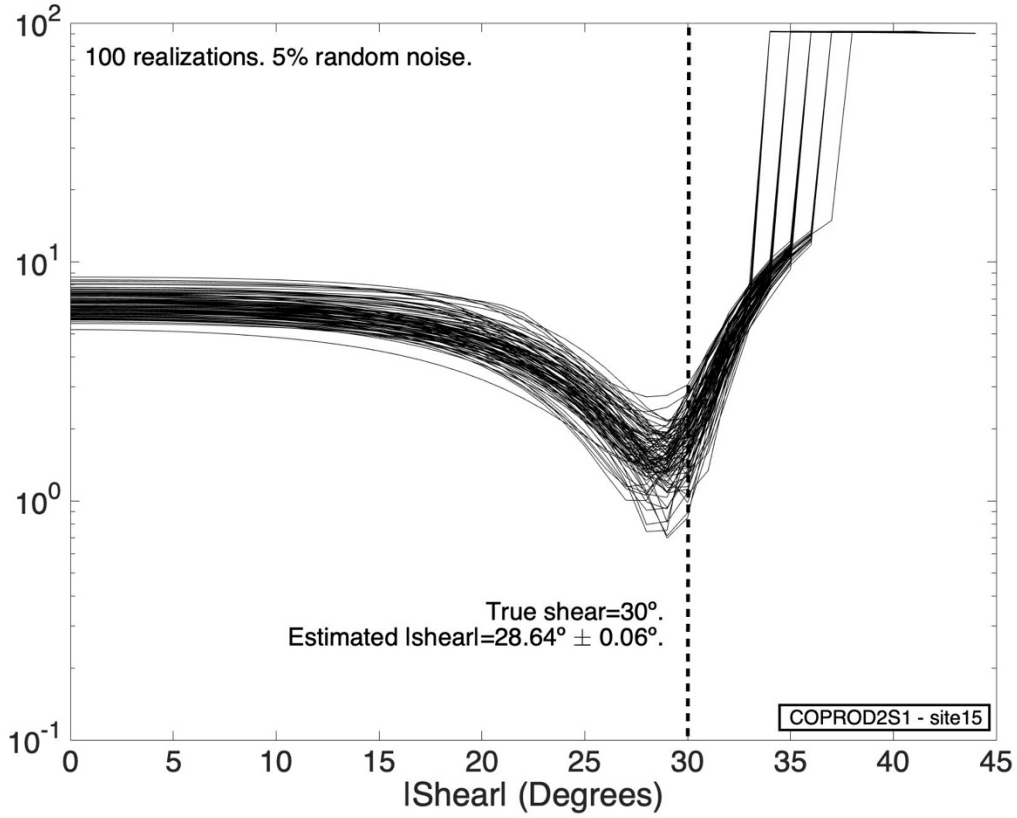

Figure 12. Estimation of the absolute value of shear comparing the phases from the quadratic equation and from the phase tensor. Both are immune to strike and to twist. The optimum absolute value of shear is the average of the corresponding minima.

We now return to the familiar ground of the previous sections. Figure 13 shows the estimation of twist assuming the plus and minus signs for the value of shear. It is very clear that the sign of shear must be positive because this allows a much better fit to the data at the optimum twist. This speaks well of the Groom-Bailey distortion model and in particular of how twist and shear are defined. The estimated twist is within a fraction of a degree from the true value. The fit to the data for both positive and negative signs of shear is shown in Figure 14. We show only the *xy* and *yx* components. It can be observed that definitively the best fit is for the positive sign. It is important to recall that what we are after here is the association of a strike with a 2x2 tensor with only two elements different

from zero. Everything relevant for interpretation is known. The only thing missing is the order of the two elements of the tensor. Shear and twist are needed only for uncovering this order. The success or failure of the process is not to be judged by the strict fit to the data. For instance, the fit for the positive sign shown in Figure 14 is far from perfect. However, the fit for negative sign is a lot worse. And it is a lot worse because it has the modes in the opposite sense: *xy* with *yx* and vice versa.

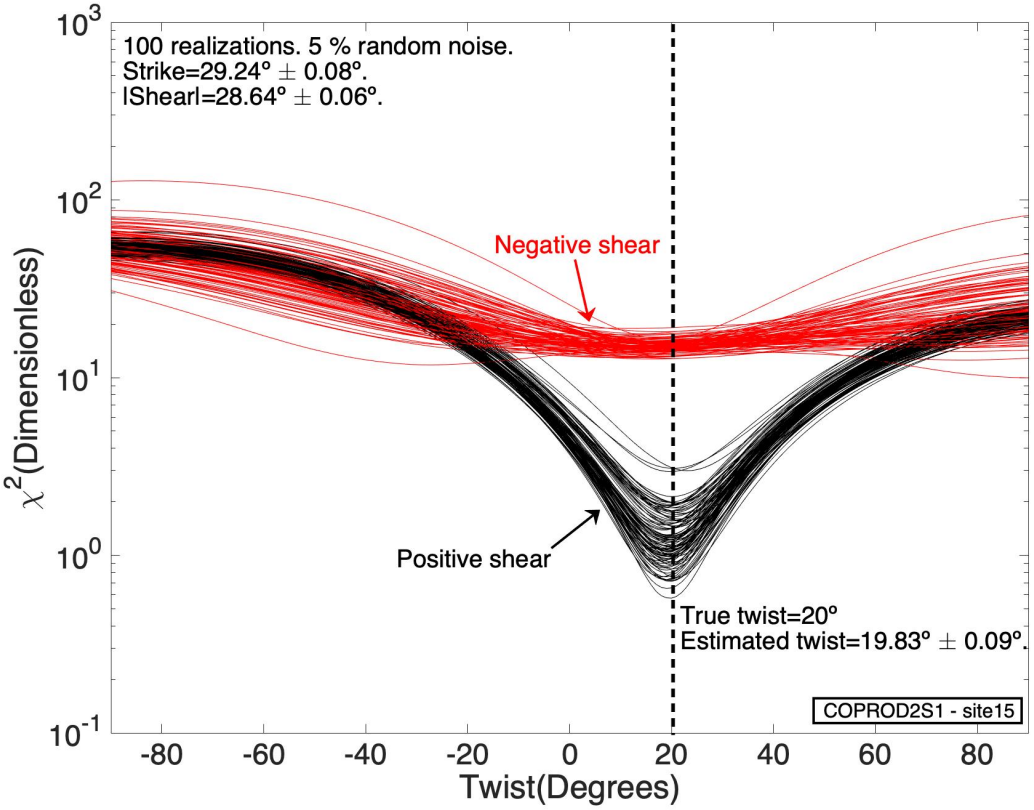

Figure 13. χ^2 objective functions for the estimation of twist assuming the two possibilities for the unknown sign of shear. It can be observed that the lowest minima correspond to the correct positive shear. The strike was set to the estimated 29 degrees and the absolute value of shear to the also estimated value of 28.64 degrees.

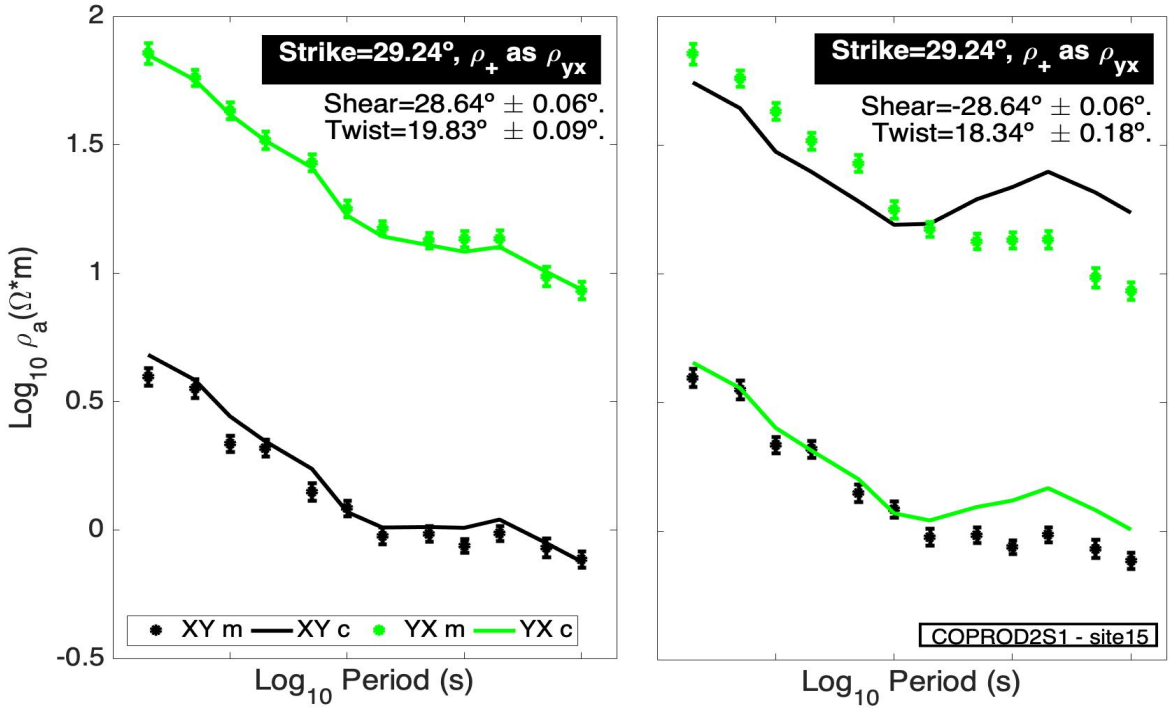

Figure 14. Comparison of the distorted data with the response of the distortion model assuming positive and negative signs for the value of shear. We present only the corresponding components xy and yx. It can be observed that the computed resistivities fall in the correct place for the positive shear.

Applications to field data

The application of the approach to field data follows the sequence of the general case discussed above. We chose site lit902 of the established BC87 dataset (e.g. Jones, 1993). The data are shown in Figure 15. It can be observed that they have a 3D character as those of Figure 8 possibly because of galvanic distortions. Clearly the impedance tensor is not symmetric.

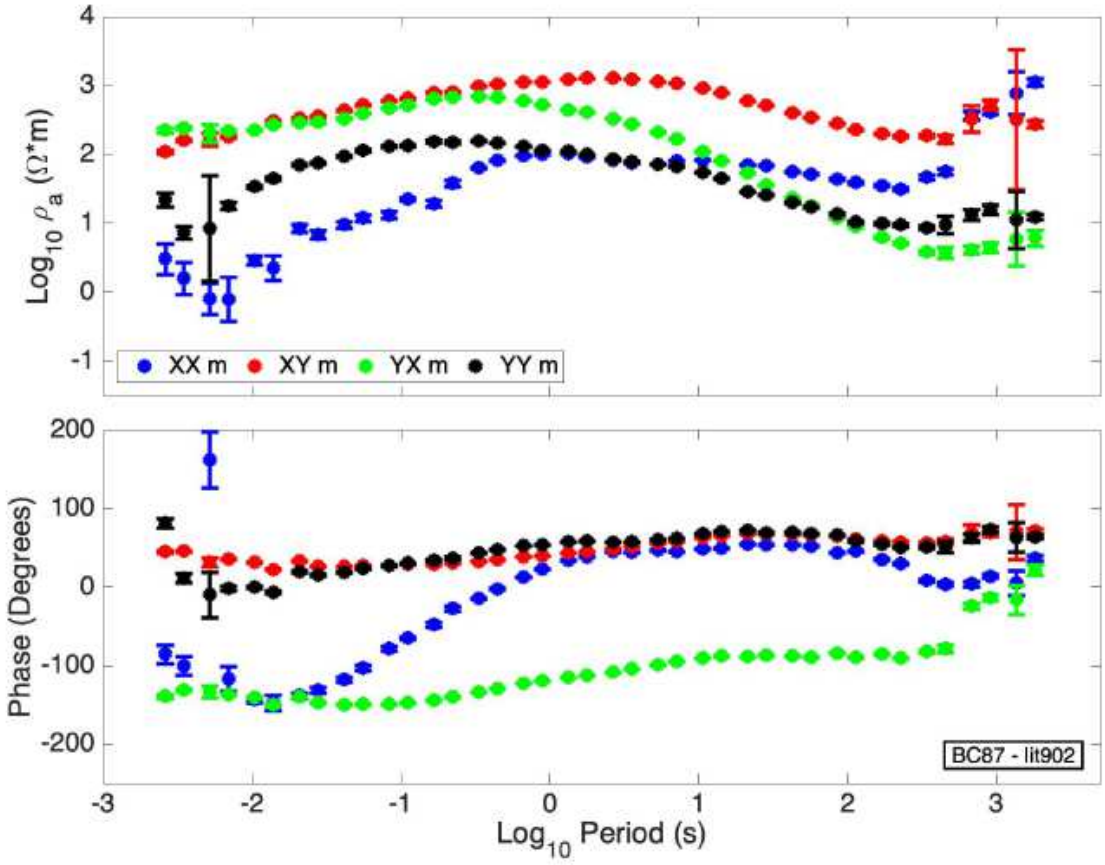

Figure 15. Data of site lit902 of the BC87 dataset.

Figure 16 shows the estimation of the strike using the same reframed versión of the phase tensor as for Figure 11. The approach is detailed in Bravo-Osuna et al., (2021). Its main feature is that it allows optimization over windows of several periods. In this case the estimate is based on using all the available periods. As mentioned befere, the penalty function depends on the strike and in 2D is the norm of the offdiagonal elements of the phase tensor. The estimate using 100 realizations is 62 degrees.

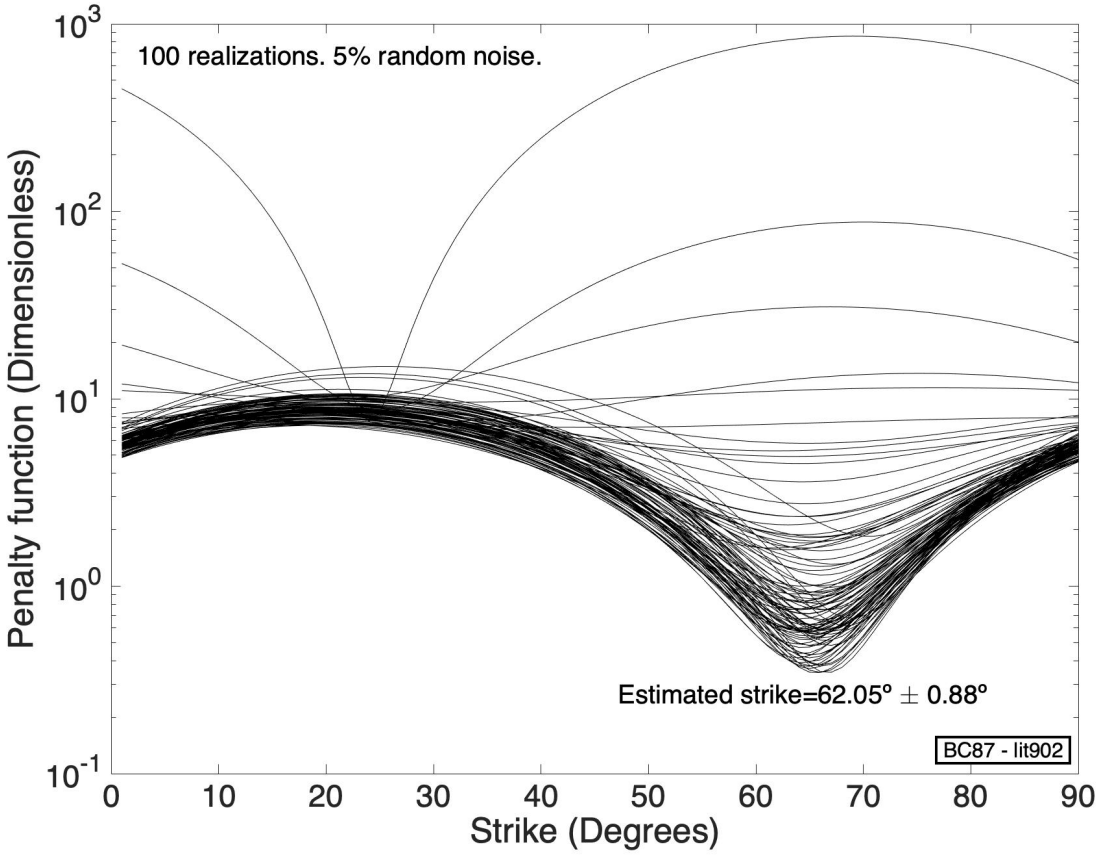

Figure 16. Estimation of strike using the reframed version of the phase tensor for a window that includes all the available periods.

We now come to the estimation of the absolute value of shear. As for Figure 12 this is also obtained through optimization. Recall that equation 4 provides phases $\varphi_{\pm}$ that depend on the square of shear and that the phases Φ_{max} and Φ_{min} from the phase tensor don't depend on shear, and reduce in 2D to the phases of the TE and TM modes. Again, the penalty function in this case is the norm of the difference between the phases of the two approaches. The penalty function depends on the absolute value of shear and in ideal

2D cases is exactly zero at the appropriate shear. The approach is detailed in Muñiz et al., (2017). The estimated value of the absolute value of shear is of 7 degrees.

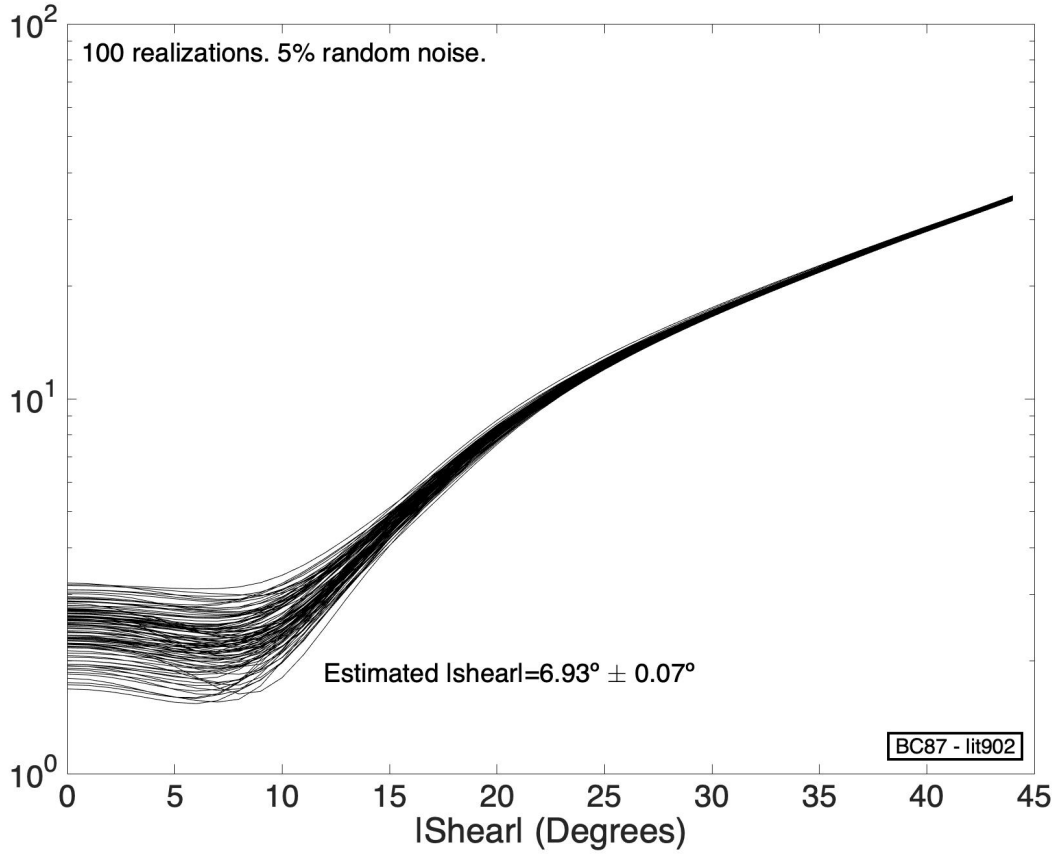

Figure 17. Estimation of the absolute value of shear comparing the phases from the quadratic equation and from the phase tensor. The optimum absolute value of shear is the average of the corresponding minima.

Figure 18 shows the estimation of twist assuming the plus and minus signs for the value of shear. This figure corresponds to Figure 13 in the previous section. The first thing to notice is that there are two minima for each sign. We think this is because we are using a single value for strike and in fact this site may require two (Muñiz et al., 2017). Still, it is

clear that the shear must be negative because in both cases the minimum corresponds to the negative shear.

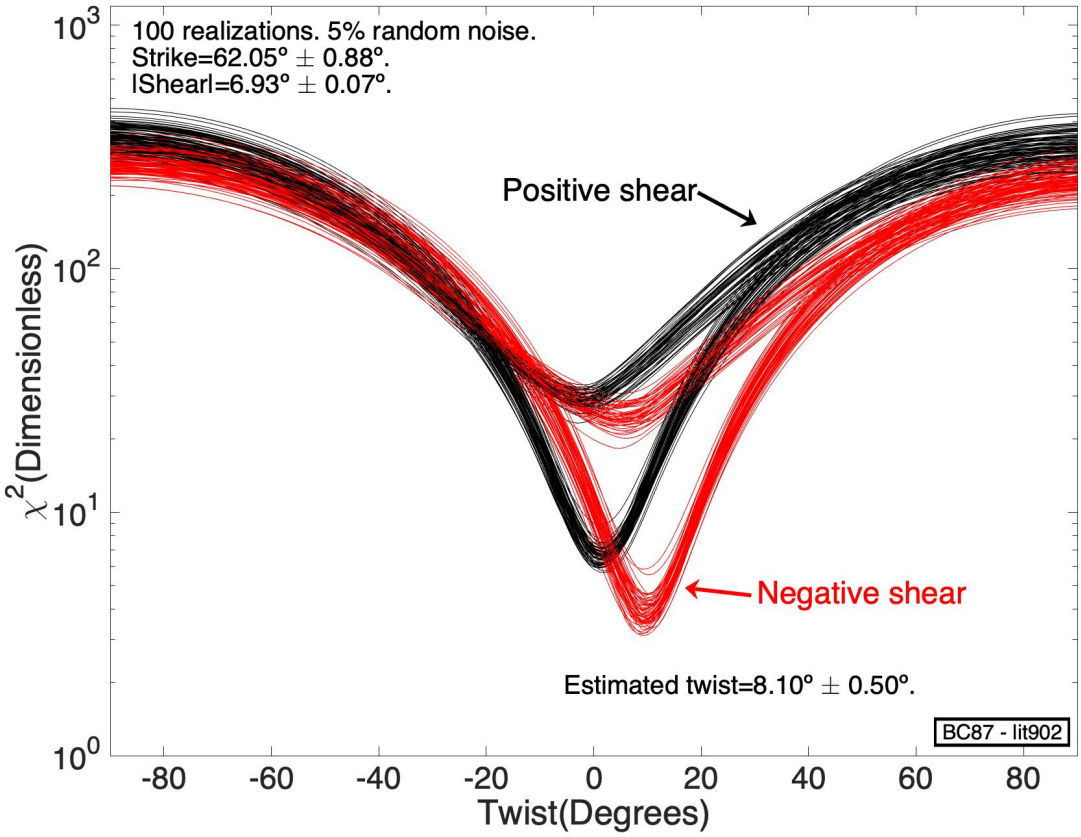

Figure 18. Site lit902 of the BC87 dataset. χ^2 objective functions for the estimation of twist assuming the two possibilities for the unknown sign of shear.

The fit to the data for both positive and negative signs of shear is shown in Figure 19. We show only the *xy* and *yx* components. It can be observed that the best fit is for the negative sign of shear. However, it must be noticed that for both signs the strike of 62 degrees indicates that hat ρ_+ must be associated with ρ_{xy}. It is important to emphasize that what we are after is the association of a strike with a 2x2 tensor that has only two

elements different from zero. Everything relevant for interpretation is known. The only thing missing is the order of the two elements of the tensor. As a final figure we present Figure 20 which summarizes the object of the exercise and indicates the output of the process: that we must identify ρ_+ with ρ_{xy}. The graphical abstract at the beginning of the paper illustrates this conclusion acknowledging the classical 90 degrees ambiguity.

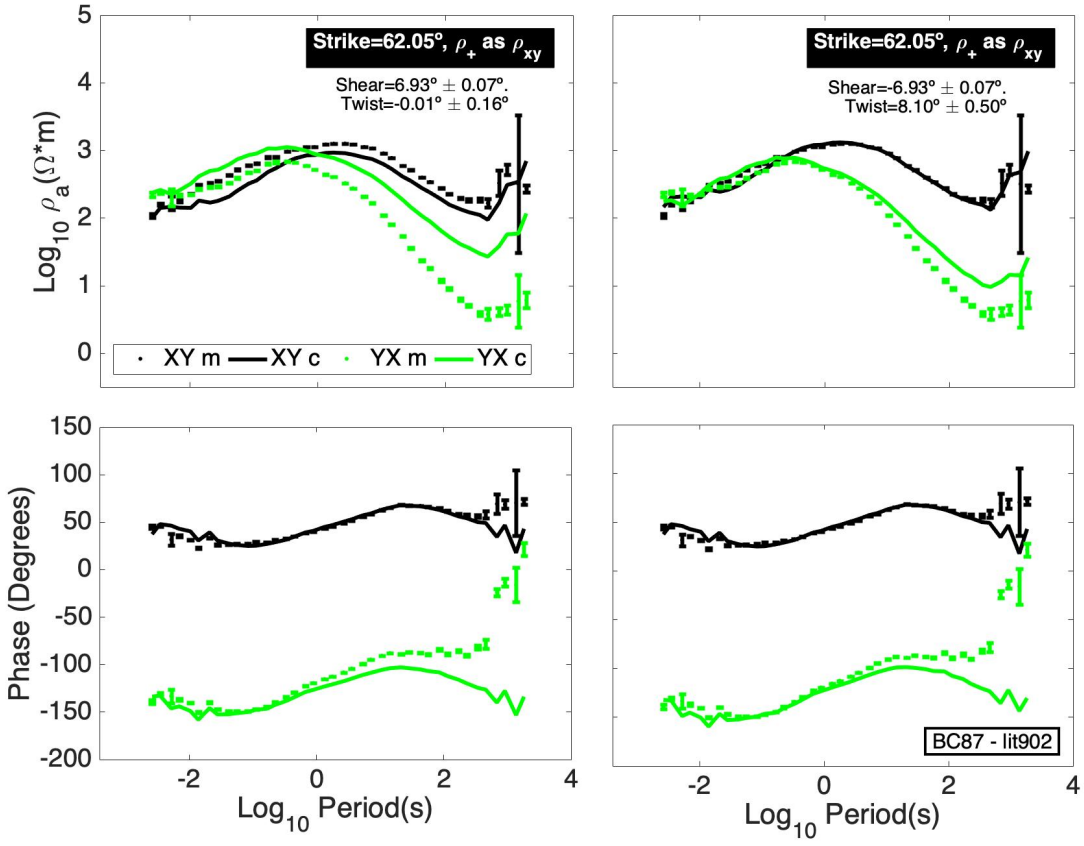

Figure 19. Site lit902 of the BC87 dataset. Comparison of the data with the response of the distortion model assuming positive and negative shears.

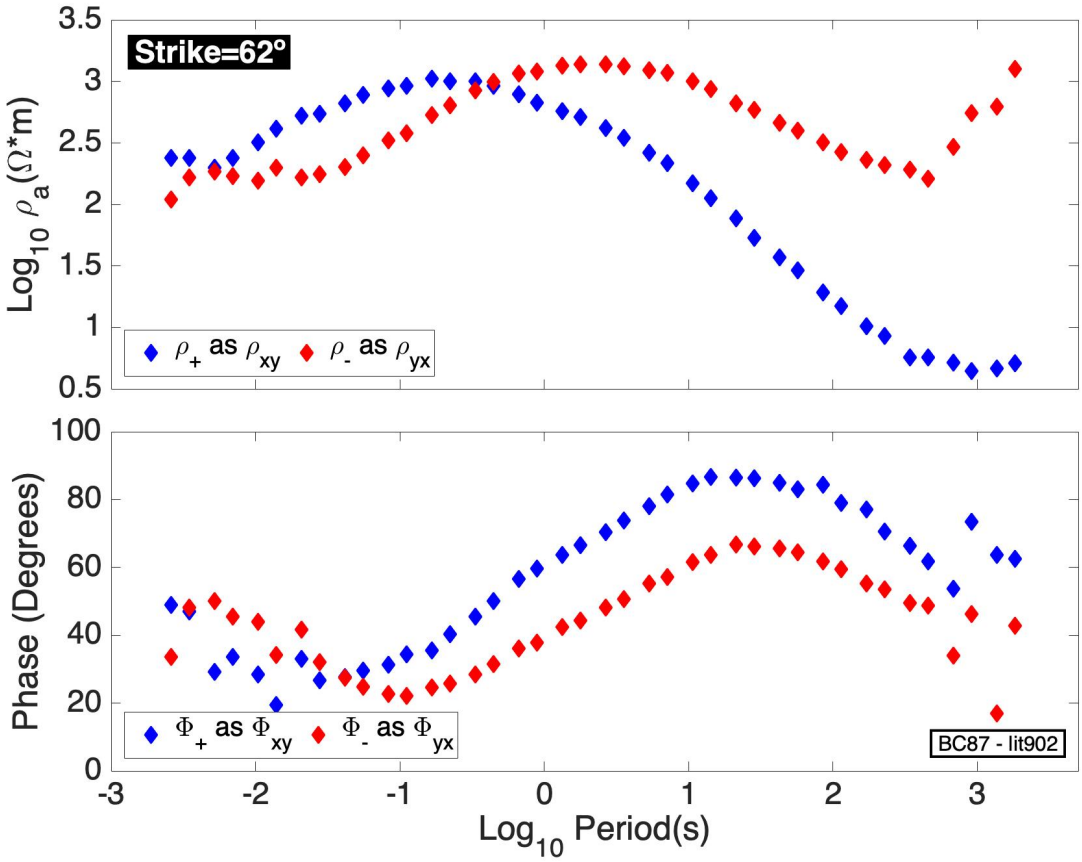

Figure 20. These graphs summarize the output of the process of linking strike angles to invariant impedances. The graphical abstract at the beginning of the article considers the classical ambiguity of 90 degrees.

CONCLUSIONS

In the Groom-Bailey distortion model all variables are interconnected and to fit the data it is necessary to recur to elaborated numerical methods. Bahr's strike angle, the phases Φ_{max} and Φ_{min} derived from the phase tensor and the impedances from the quadratic equation can be thought of as partial solutions for the Groom-Bailey distortion model. The analytical or semi-analytical nature of these solutions is their main asset. However, their full usage can be severely limited because in the process of breaking the

problem into sub-problems, the solutions decouple from each other. The quadratic equation and the phases Φ_{max} and Φ_{min} are invariant under rotation which means that they are decoupled from the strike angle. We can obtain the impedances but do not know to which angle they belong, even if we know the angles. This is in addition to the classical ambiguity of ninety degrees. It is actually a binary question of this or that. It is important because the association strike-impedances provides the physical link with the local geology. Bringing back the original distortion model is the only way to reestablish the connection. Our results show that this link reduces to a binary decision by inserting the partial calculations into the original decomposition. The process requires the optimization of only the distorting parameter twist. Nevertheless, this has to be done twice because the sign of shear is the other unknown. We do not look for the full optimization of the problem as does the algorithm STRIKE. In fact, we believe nothing can fit the data better than this algorithm. The missing link between strikes and impedances needed only a binary answer and this is what the proposed approach provides.

Availability of data and materials

The COPROD2S1 dataset is available at the MTNet site (https://www.mtnet.info/workshops/mt-diw/mt-diw4/mt-diw4.html). The BC87 dataset is available at the MTNet site (http://www.complete-mt-solutions.com/mtnet/main) . A Matlab code for the computation of all the parameters is available from the corresponding author upon request.

Abbreviations

MT: Magnetotelluric; 2D: Two-dimensional; 3D: Three-dimensional; TE: Transverse electric; TM: Transverse magnetic.

Acknowledgements

R.F.A-C acknowledge scholarships from CONACYT for their graduate work at CICESE. The authors also thank the anonymous reviewers for fruitful comments to improve the clarity of the paper.

Author details
Departamento de Geofísica Aplicada, División de Ciencias de la Tierra, CICESE, 22860 Ensenada, Baja California, México.

Authors' contributions
All the authors contributed about equally to this work. All the authors read and approved the final manuscript.

Competing interests
The authors declare that they have no competing interests.

Funding
CICESE and CONACyT.

REFERENCES

Bahr, K., 1988. Interpretation of the magnetotelluric impedance tensor: regional induction and local telluric distortion, *J. Geophys.,* **62,** 119-127.

Bostick, FX., 1984. Electromagnetic array profiling survey method: U.S. patent 4,591,791.

Bostick, FX., 1986. Electromagnetic array profiling: 56th Annual International Meeting, SEG, Expanded Abstracts, pp 60–61.

Bravo-Osuna, A.G., Gómez-Treviño, E., Cortés-Arroyo, O.J., Delgadillo-Jauregui, N.F. and Arellano-Castro R.F., 2021. Reframing the magnetotelluric phase tensor for monitoring applications: improved accuracy and precision in strike determinations. Earth, Planets and Space 73:34.

Caldwell, T.G., Bibby, H.M., Brown, C. 2004. The magnetotelluric phase tensor. Geophys J Int 158:457–469.

Gómez-Treviño E., Romo J.M., Esparza F.J. 2014a. Quadratic solution for the 2-D magnetotelluric impedance tensor distorted by 3-D electro-galvanic effects. Geophys J Int 198:1795–180.

Gómez-Treviño E, Esparza F, Muñiz Y, Calderón A. 2014b. The magnetotelluric transverse electric mode as a natural filter for static effects: application to the COPROD2 and COPROD2S2 data sets. Geophysics 79:E91–E99.

Gómez-Treviño, E., Muñiz Gallegos, Y., Cuellar Urbano, M., & Calderón Moctezuma, A. 2018. Invariant TE and TM magnetotelluric impedances: Aplication to the BC87 dataset. Earth, Planets and Space, 70, 133-147.

Groom, R.W. and Bahr, K. 1992. Corrections for near surface effects: decomposition of the magnetotelluric impedance tensor and scaling corrections for regional resistivities: a tutorial, *Surv. Geophys.,* 13, 341- 380.

Groom, R.W. and Bailey, R.C.1989. Decomposition of magnetotelluric impedance tensors in the presence of local three-dimensional galvanic distortion, *J. Geophys. Res.,* 94, 1913-1925.

Jones, A. G., 1993. The BC87 dataset: Tectonic setting, previous EM results and recorded MT data: Journal of Geomagnetism and Geoelectricity,45, 1089–1105, doi: 10.5636/jgg.45.1089.

Jones, A. G. and Groom, R. W. 1993. Strike angle determination from the magnetotelluric tensor in the presence of noise and local distortion: rotate at your peril!, *Geophys. J. Int.,* 113, 524-534.

Jones, A. G. 2012. Distortion decomposition of the magnetotelluric impedance tensors from a one-dimensional anisotropic Earth **.** *Geophys. J. Int.* 189, 268–284**.**

McNeice, G.W. and Jones, A.G. 2001. Multisite, multifrequency tensor decomposition of magnetotelluric data. Geophysics 66:158–173.

Montiel-Álvarez, A. Romo-Jones, J.M., Constable, S., and Gómez-Treviño, E. 2020. Invariant TE and TM impedances in the marine magnetotelluric method. Geophysical Journal International 221(1):163-177.

Muñíz Y., Gómez-Treviño E., Esparza F.J., Cuellar M. 2017. Stable 2D magnetotelluric strikes and impedances via the phase tensor and the quadratic equation. Geophysics 82(4):E169–E186.

Swift, C.M. 1967. A magnetotelluric investigation of an electrical conductivity anomaly in the southwestern United States. Doctoral Dissertation, Massachusetts Institute of Technology.

Varentsov, I.M. 1998. 2D synthetic data sets COPROD-2S to study MT inversion techniques. In: The 14th workshop on electromagnetic induction in the Earth, Sinaia, Romania.

Figures

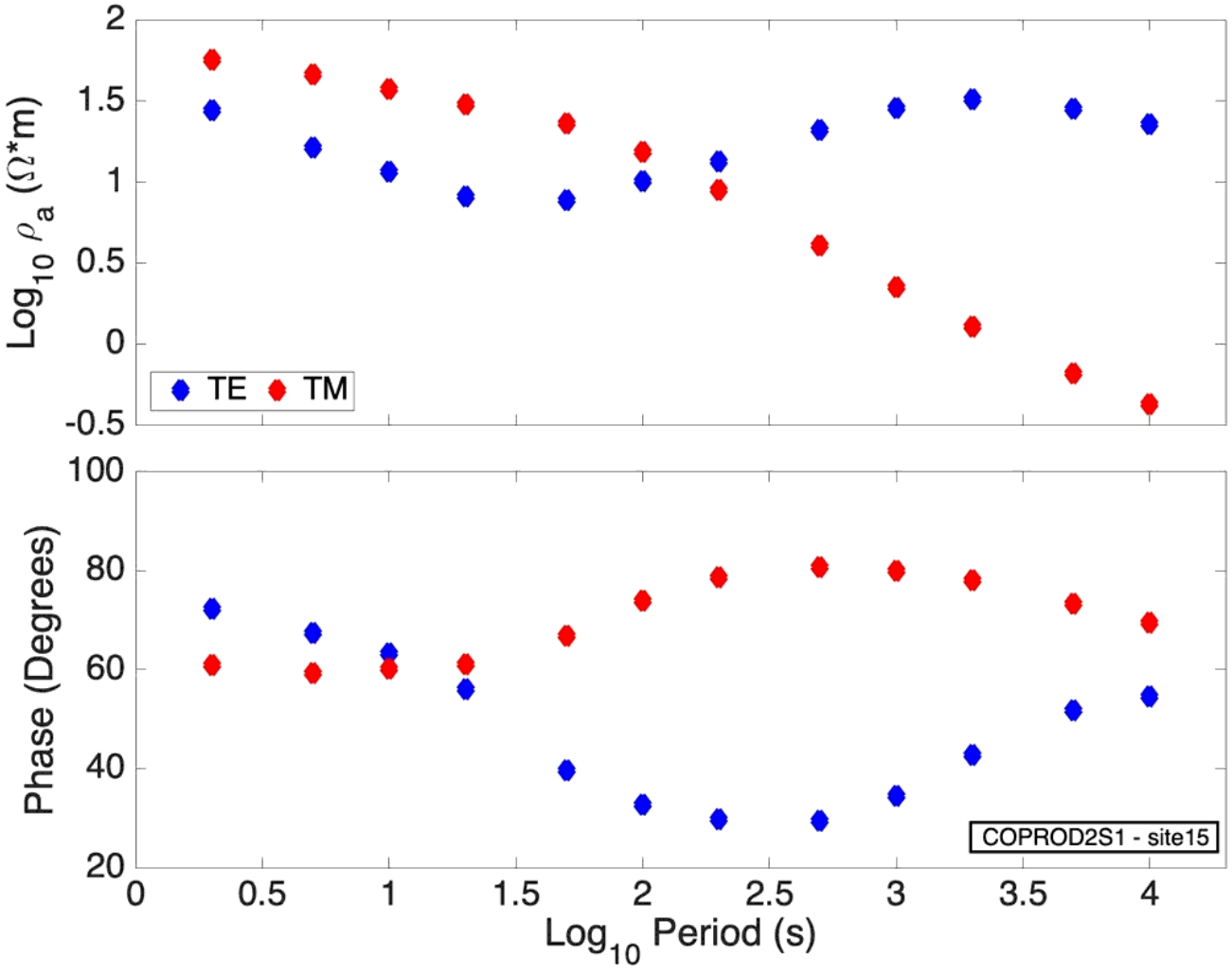

Figure 1

The original apparent resistivity and phase curves of the site 15 from the COPROD2S1 dataset. These curves are the objective of the recovery process from distorted versions of them.

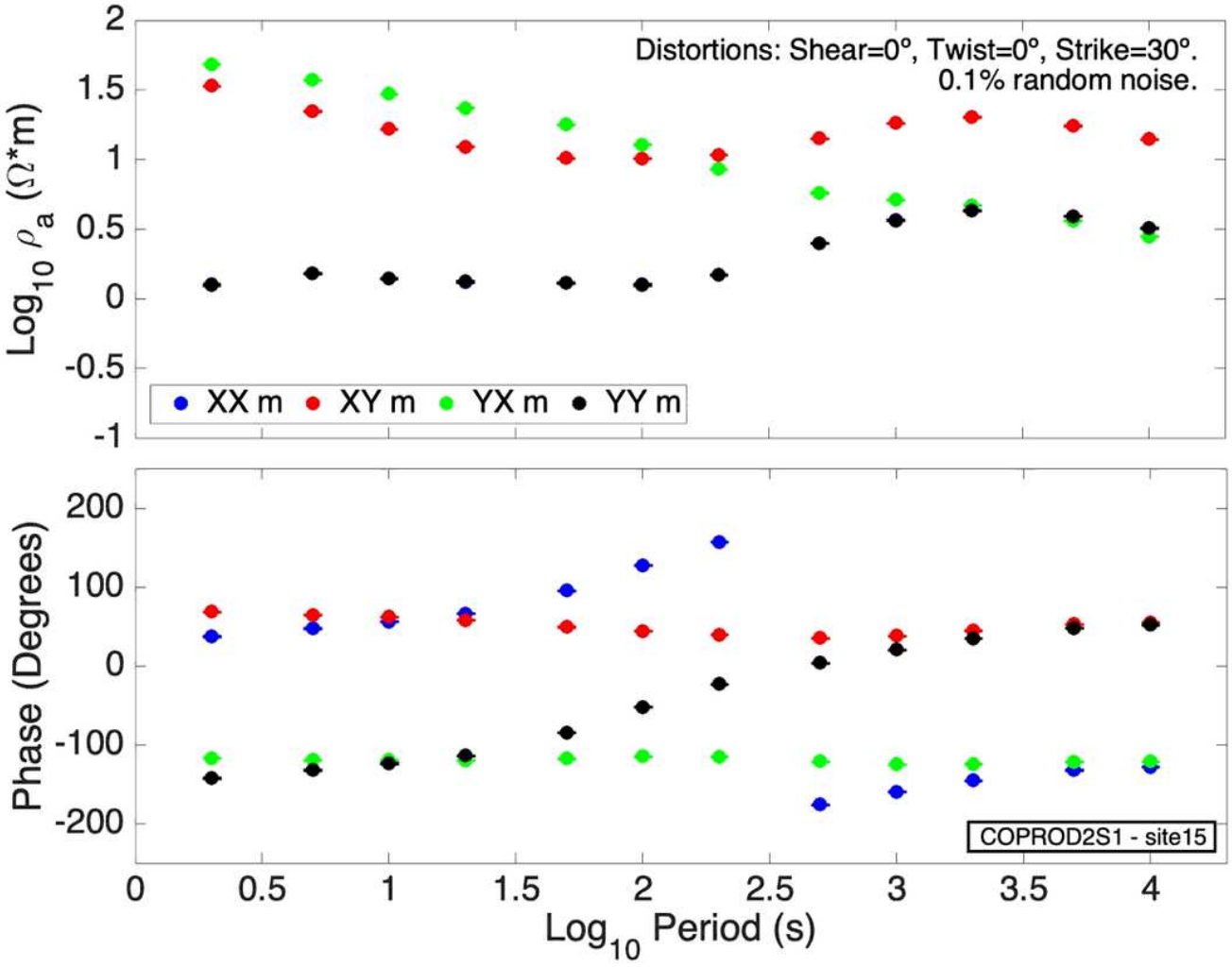

Figure 2

Distorted apparent resistivity and phase curves of site 15 from the COPROD2S1 dataset. These curves are the input for the process whose objective is the recovery of the undistorted curves of Figure 1. The distorting parameters are strike 30, twist 0 and shear 0 degrees. The random noise is 0.1 %.

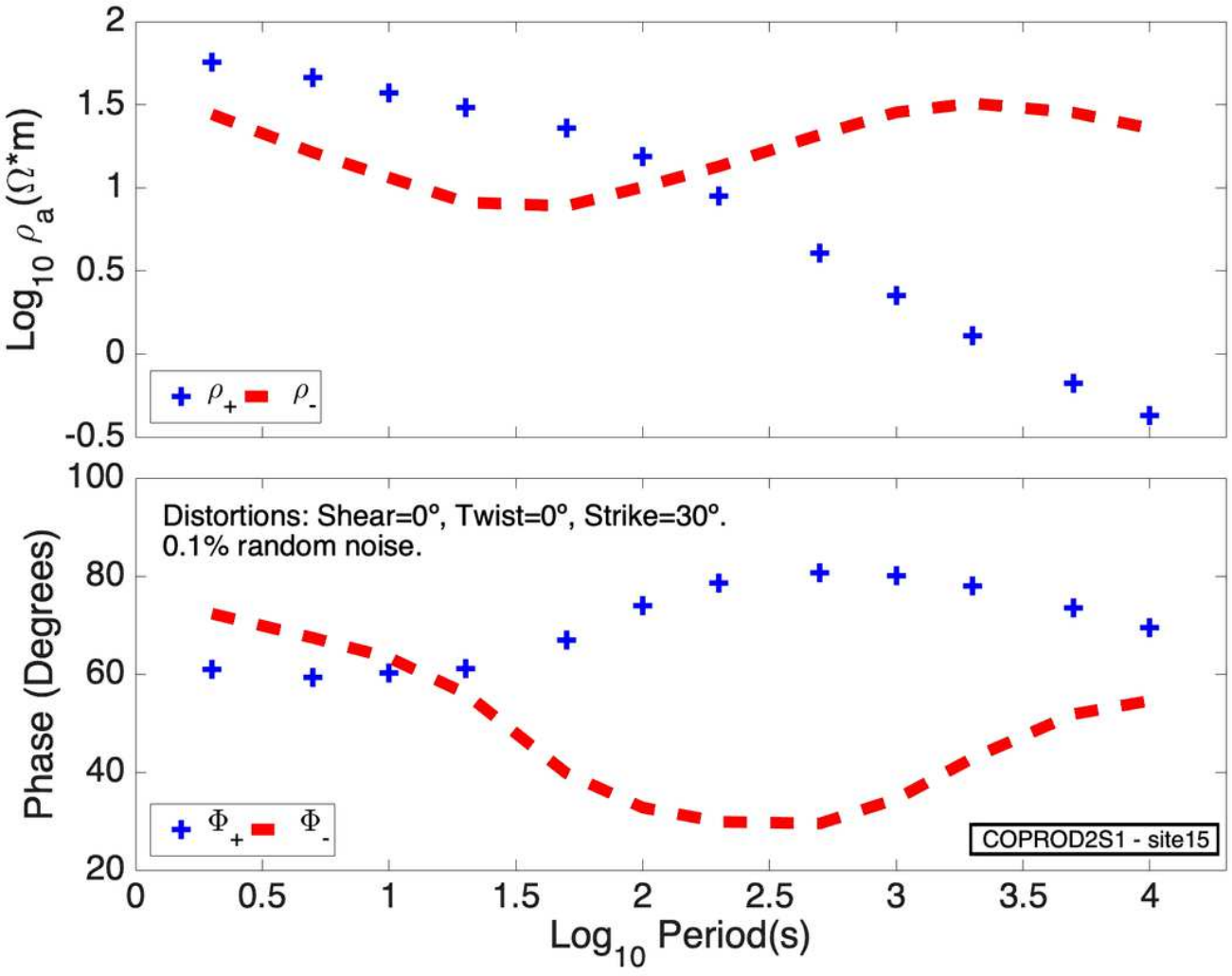

Figure 3

Recovered apparent resistivities ρ_± and phases ⍰_± through the application of the quadratic equation. Notice that the curves are the same as the original ones. However, in this case we lose track of the strike because the quadratic equation provides invariant values under rotation.

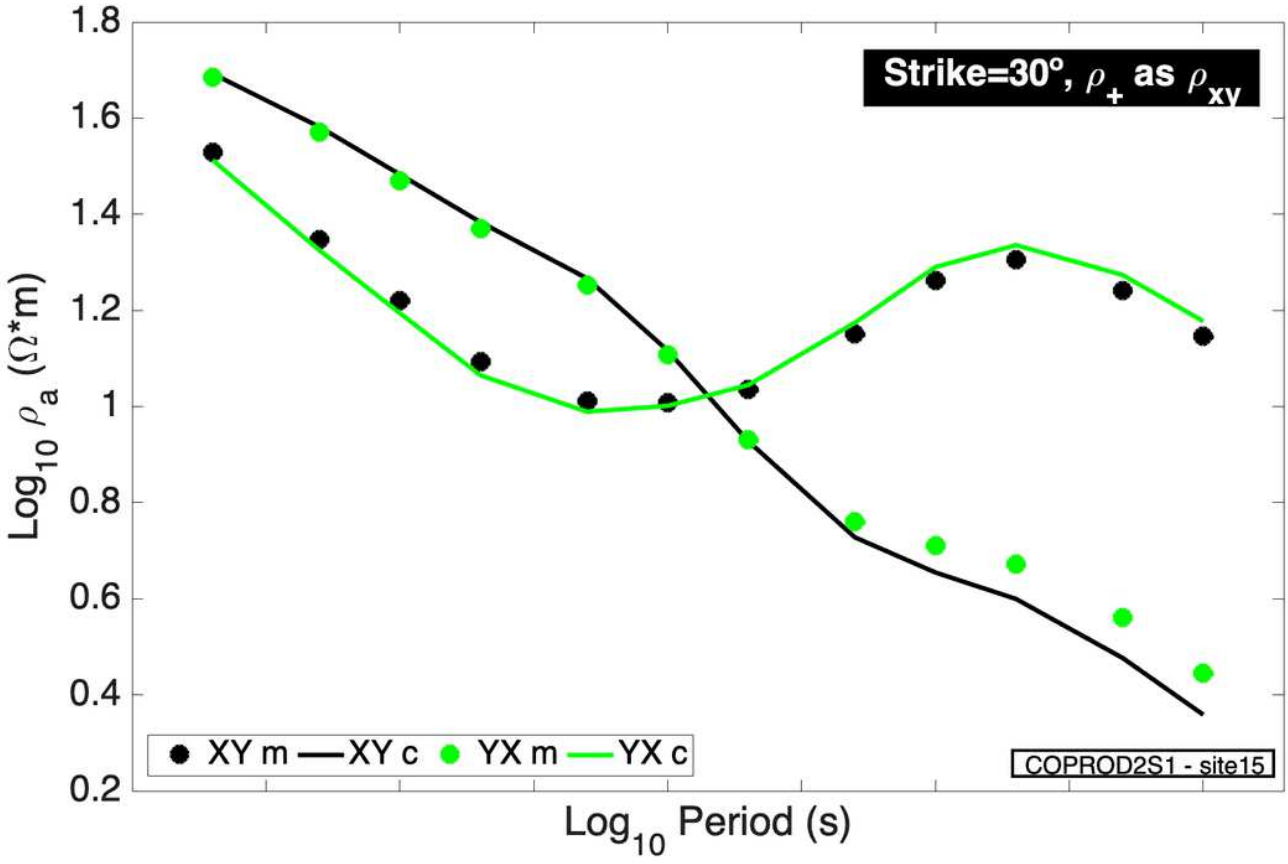

Figure 4

Comparison of the distorted data with the response of the distortion model assuming that ρ_+ is ρ_xy and a strike of 30 degrees. We present only the corresponding components xy and yx. It can be observed that the computed resistivities fall in the reverse sense as expected if the hypothesis was to hold. This means that we should identify a strike of 30 degrees with ρ_+ as ρ_yx.

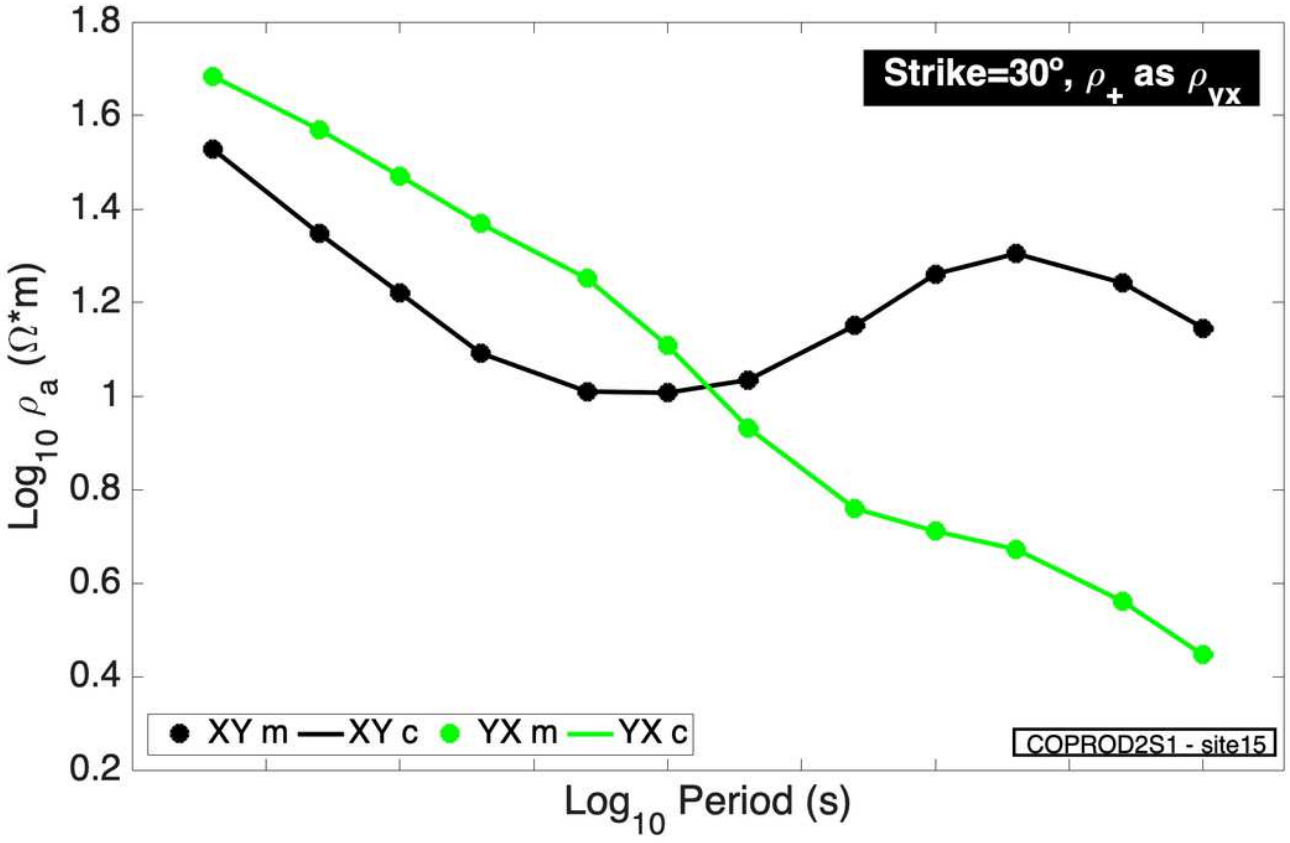

Figure 5

Comparison of the distorted data with the response of the distortion model assuming that ρ_+ is ρ_yx and a strike of 30 degrees. We present only the corresponding components xy and yx. It can be observed that the computed resistivities fall in the correct sense. This means that we should identify a strike of 30 degrees with ρ_+ as ρ_yx.

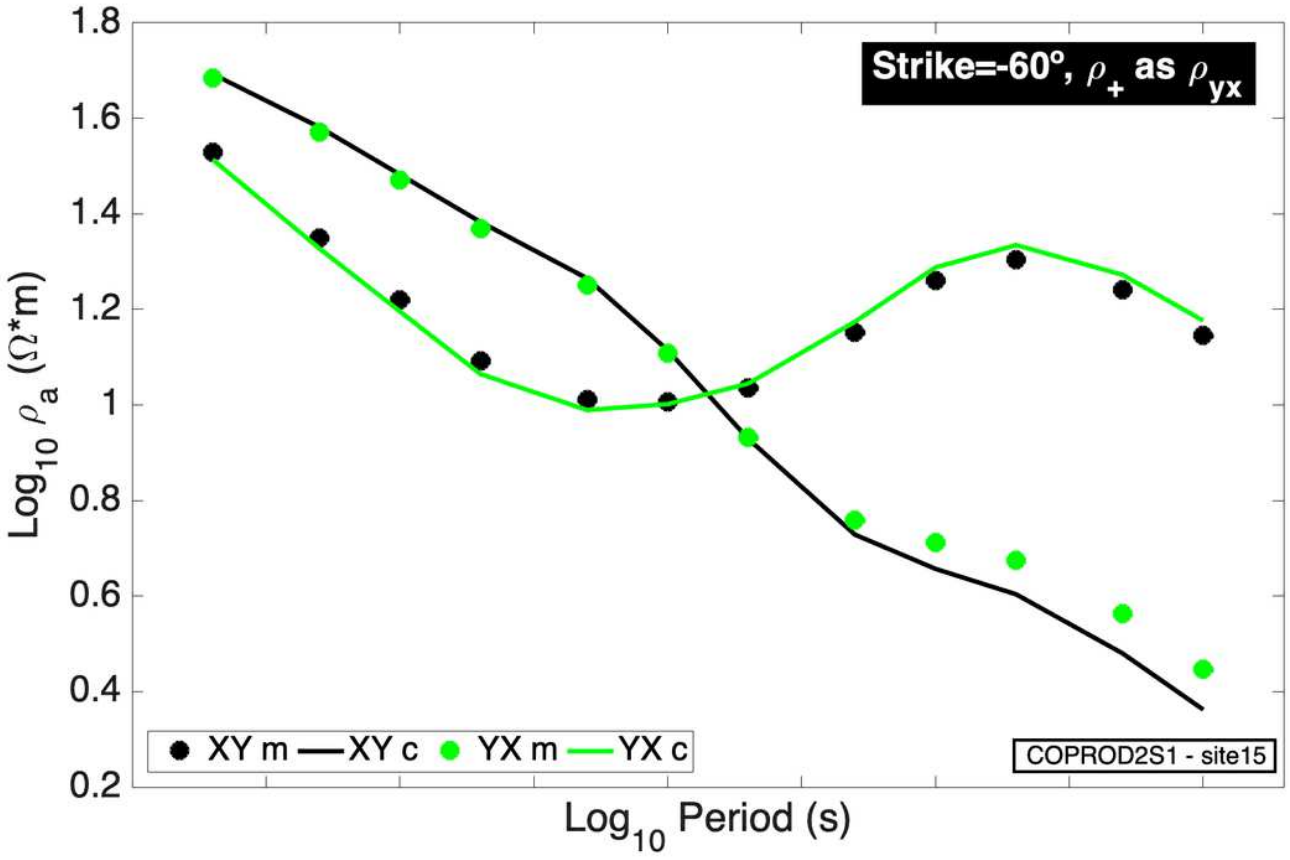

Figure 6

Comparison of the distorted data with the response of the distortion model assuming that ρ_+ is ρ_yx and a strike of -60 degrees. We present only the corresponding components xy and yx. It can be observed that the computed resistivities fall in the reverse sense as expected if the hypothesis was to hold. This means that we should identify a strike of -60 degrees with ρ_+ as ρ_xy. This is equivalent to the conclusion derived from Figure 4.

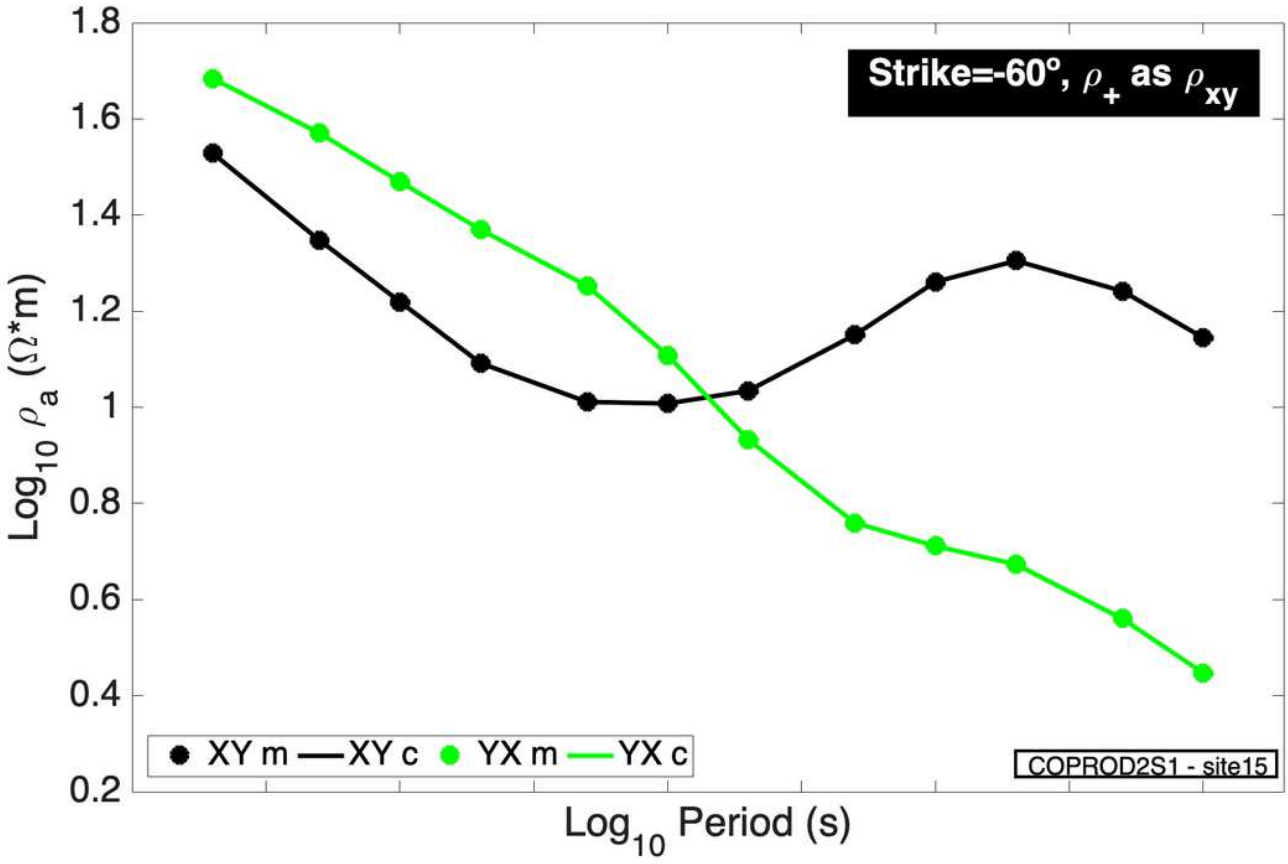

Figure 7

Comparison of the distorted data with the response of the distortion model assuming that ρ_+ is ρ_xy and a strike of -60 degrees. We present only the corresponding components xy and yx. It can be observed that the computed resistivities fall in the correct sense. This means that we should identify a strike of -60 degrees with ρ_+ as ρ_xy. This is equivalent to the conclusion derived from Figure 4.

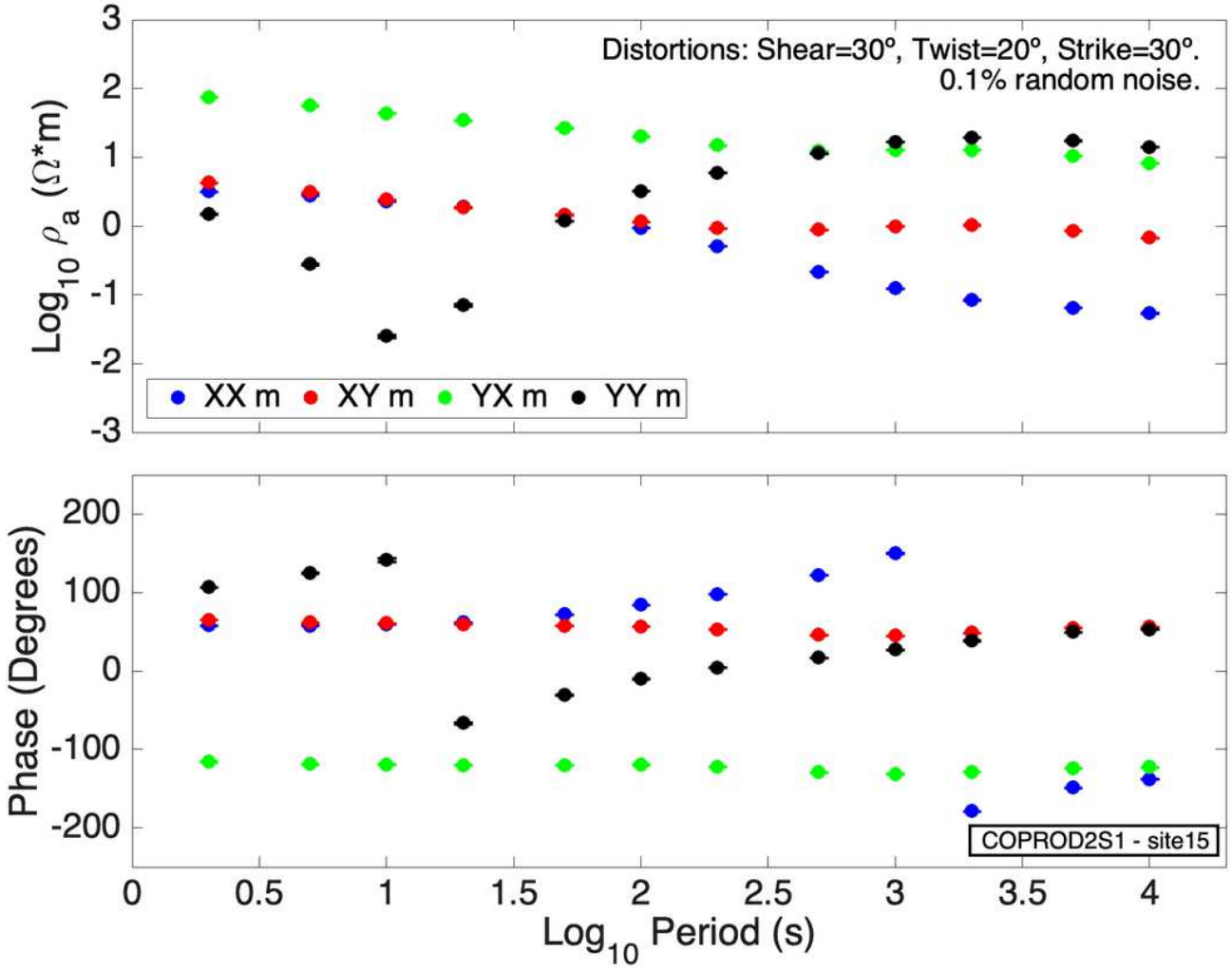

Figure 8

Distorted apparent resistivity and phase curves of site 15 from the COPROD2S1 dataset. These curves are the input of the process whose objective is the recovery of the undistorted curves of Figure1. The distorting parameters are strike 30, twist 20 and shear 30 degrees. The random noise is 0.1 %.

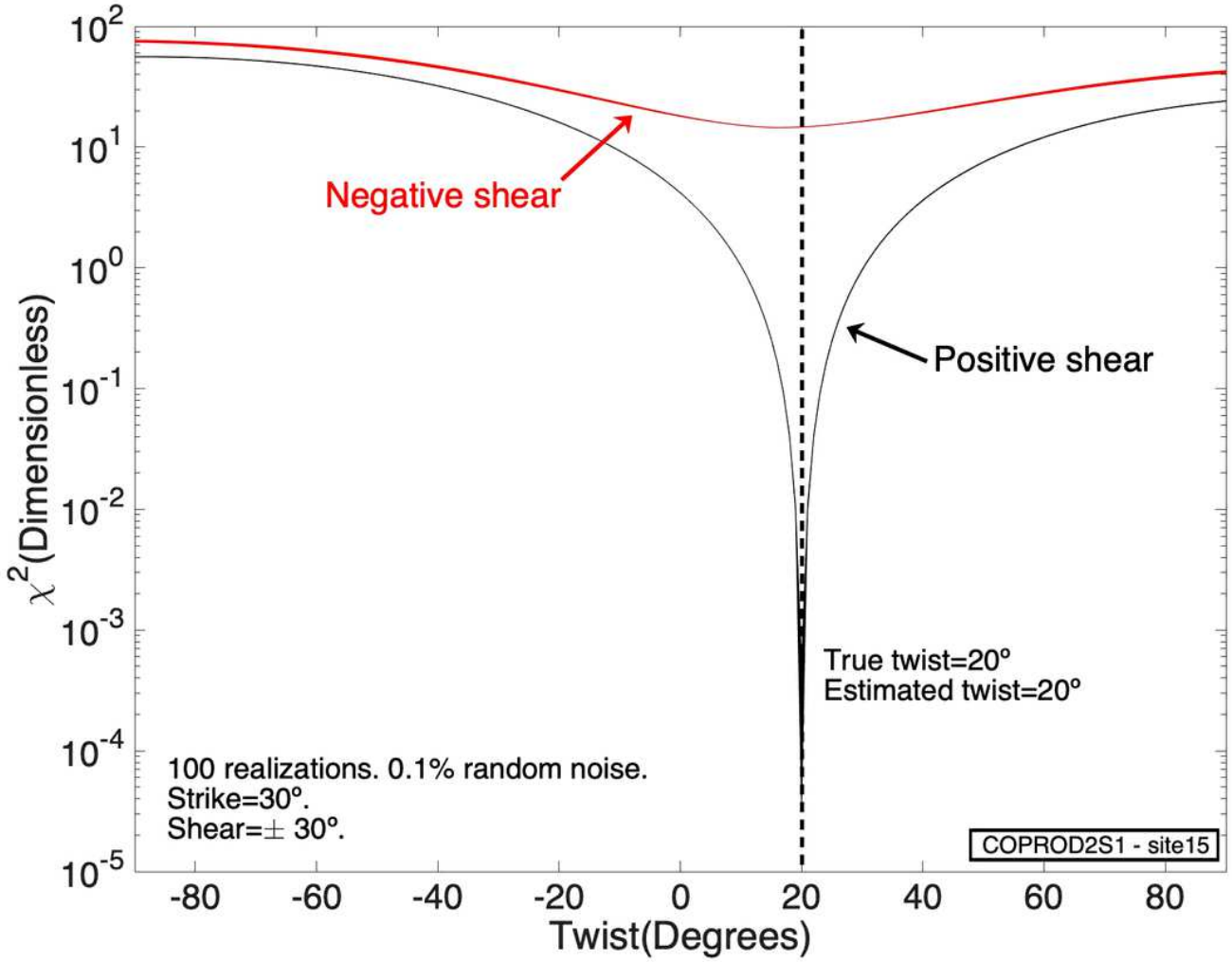

Figure 9

χ^2objective functions for the estimation of twist assuming the two possibilities for the unknown sign of shear. It can observed that the lowest minimum corresponds to the correct positive shear.

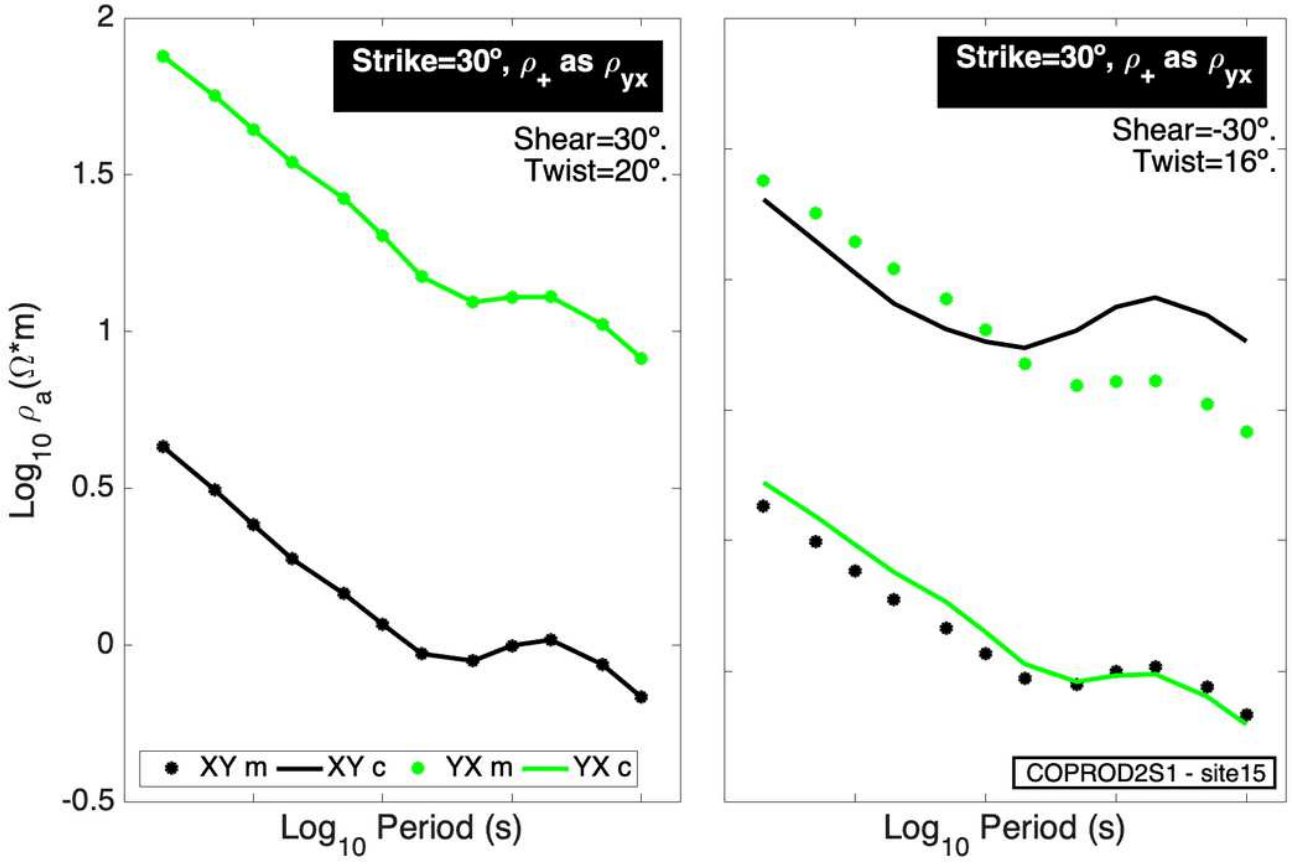

Figure 10

Comparison of the distorted data with the response of the distortion model assuming positive and negative signs for the value of shear and a twist value of 20 degrees.. We present only the corresponding components xy and yx. It can be observed that the computed resistivities fall in the correct place for the positive shear.

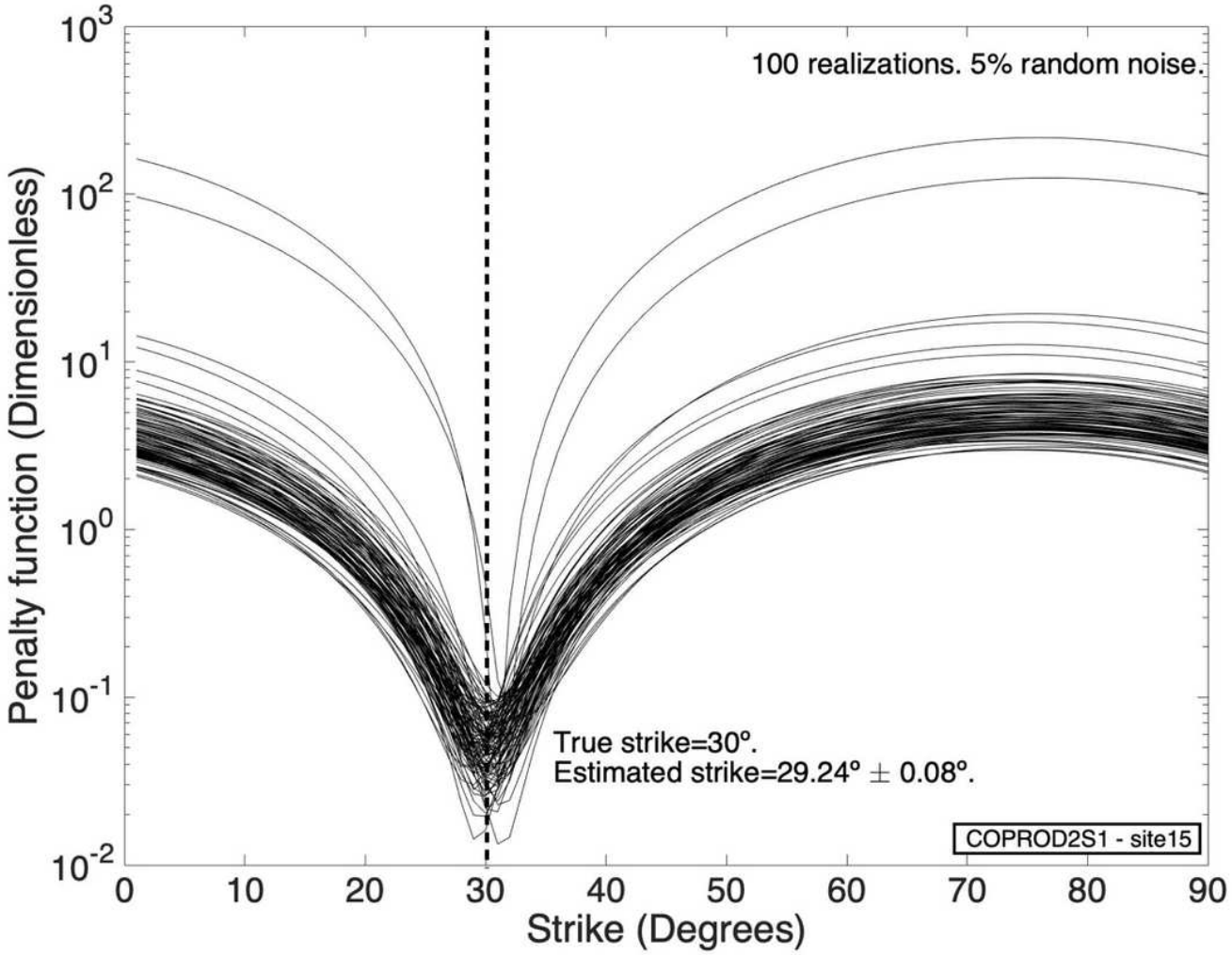

Figure 11

Estimation of strike using a reframed version of the phase tensor for a window of all 12 periods.

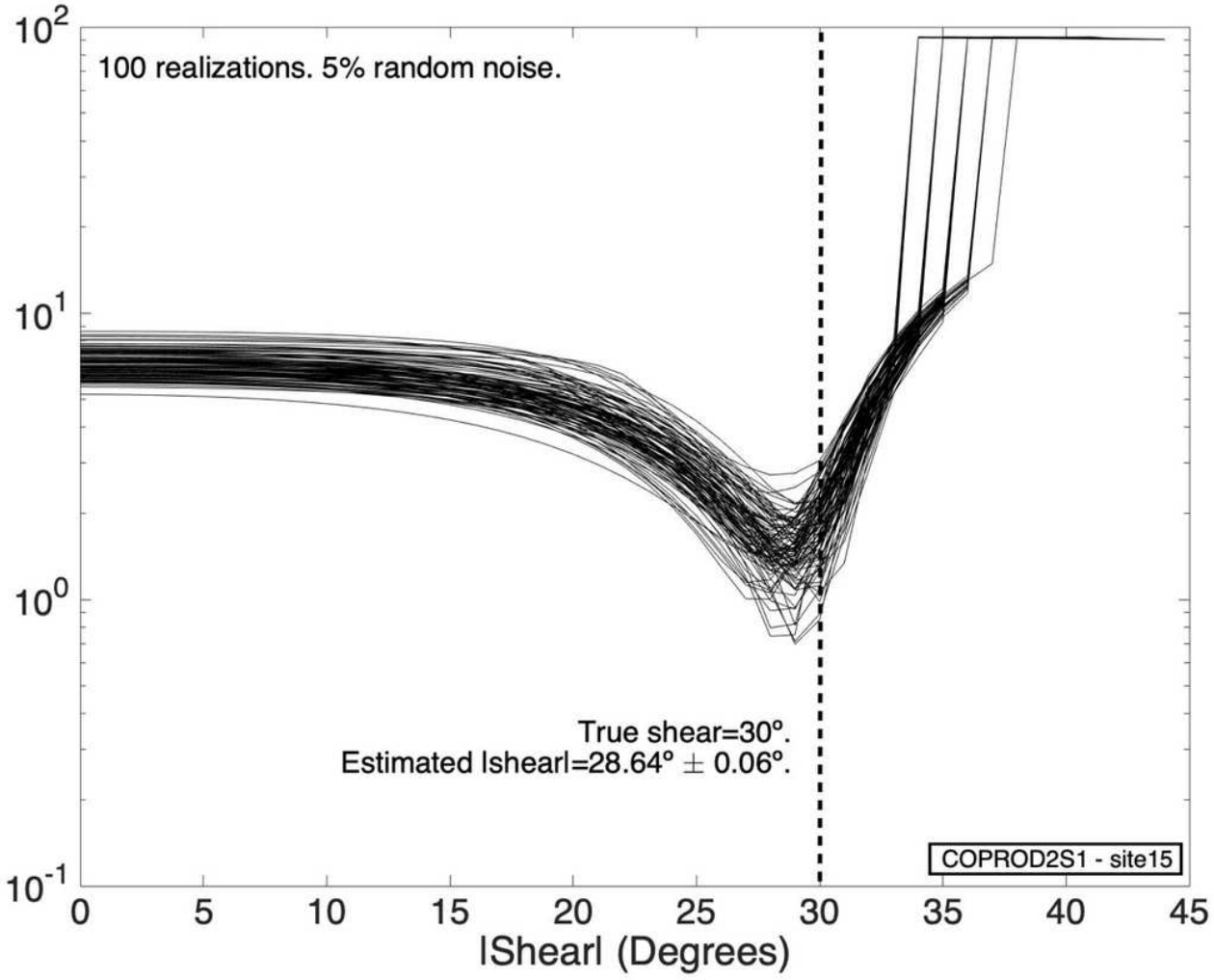

Figure 12

Estimation of the absolute value of shear comparing the phases from the quadratic equation and from the phase tensor. Both are immune to strike and to twist. The optimum absolute value of shear is the average of the corresponding minima.

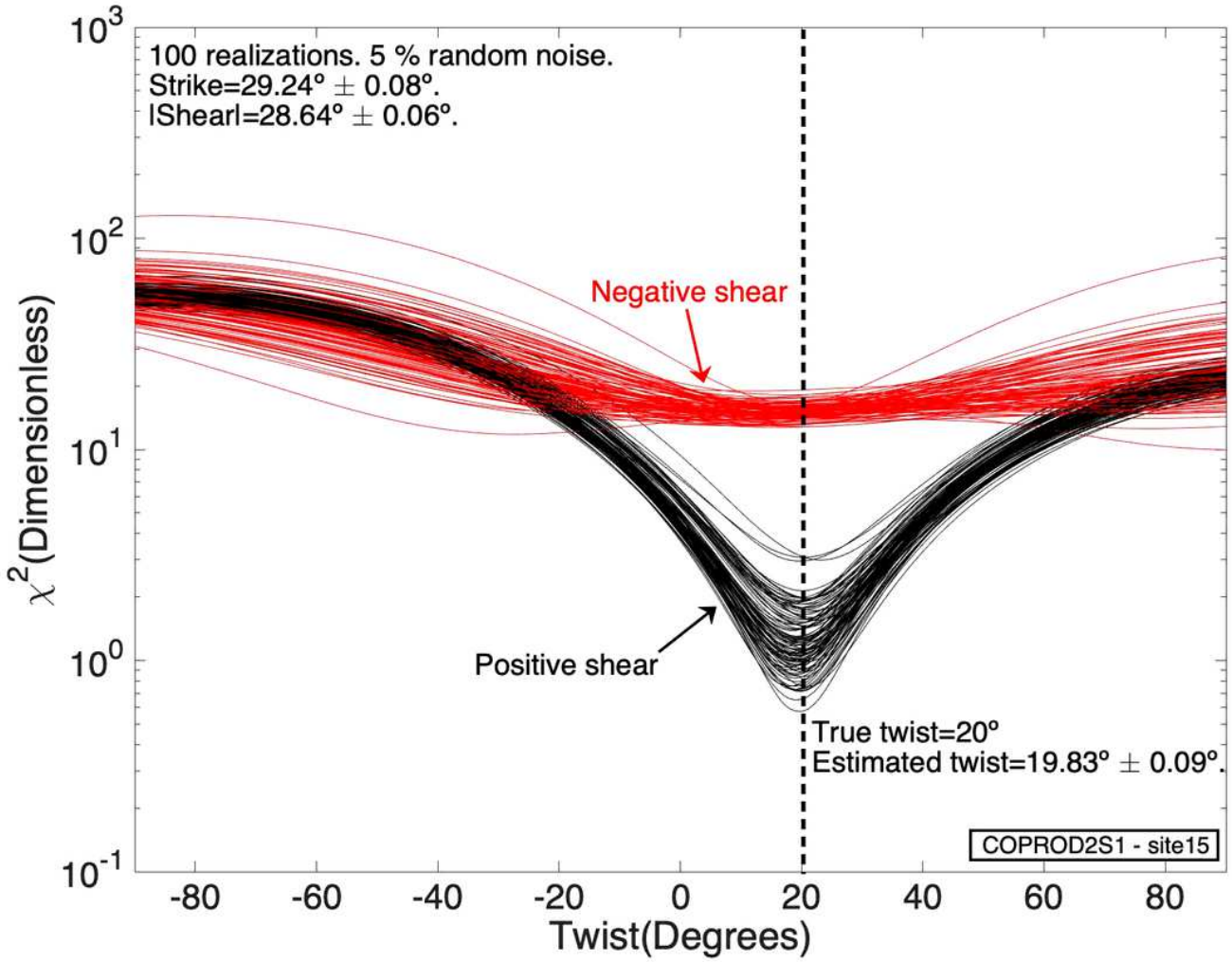

Figure 13

χ^2 objective functions for the estimation of twist assuming the two possibilities for the unknown sign of shear. It can be observed that the lowest minima correspond to the correct positive shear. The strike was set to the estimated 29 degrees and the absolute value of shear to the also estimated value of 28.64 degrees.

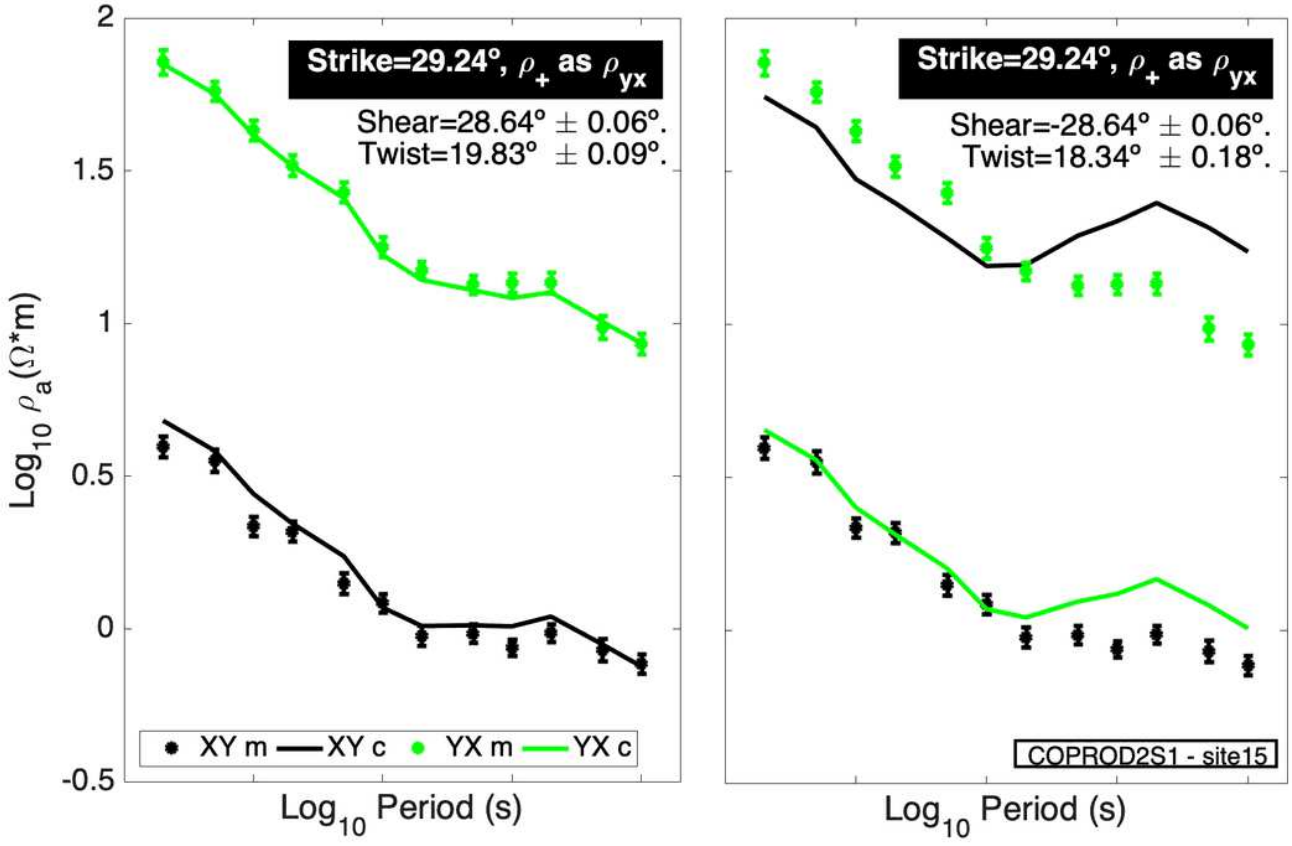

Figure 14

Comparison of the distorted data with the response of the distortion model assuming positive and negative signs for the value of shear. We present only the corresponding components xy and yx. It can be observed that the computed resistivities fall in the correct place for the positive shear.

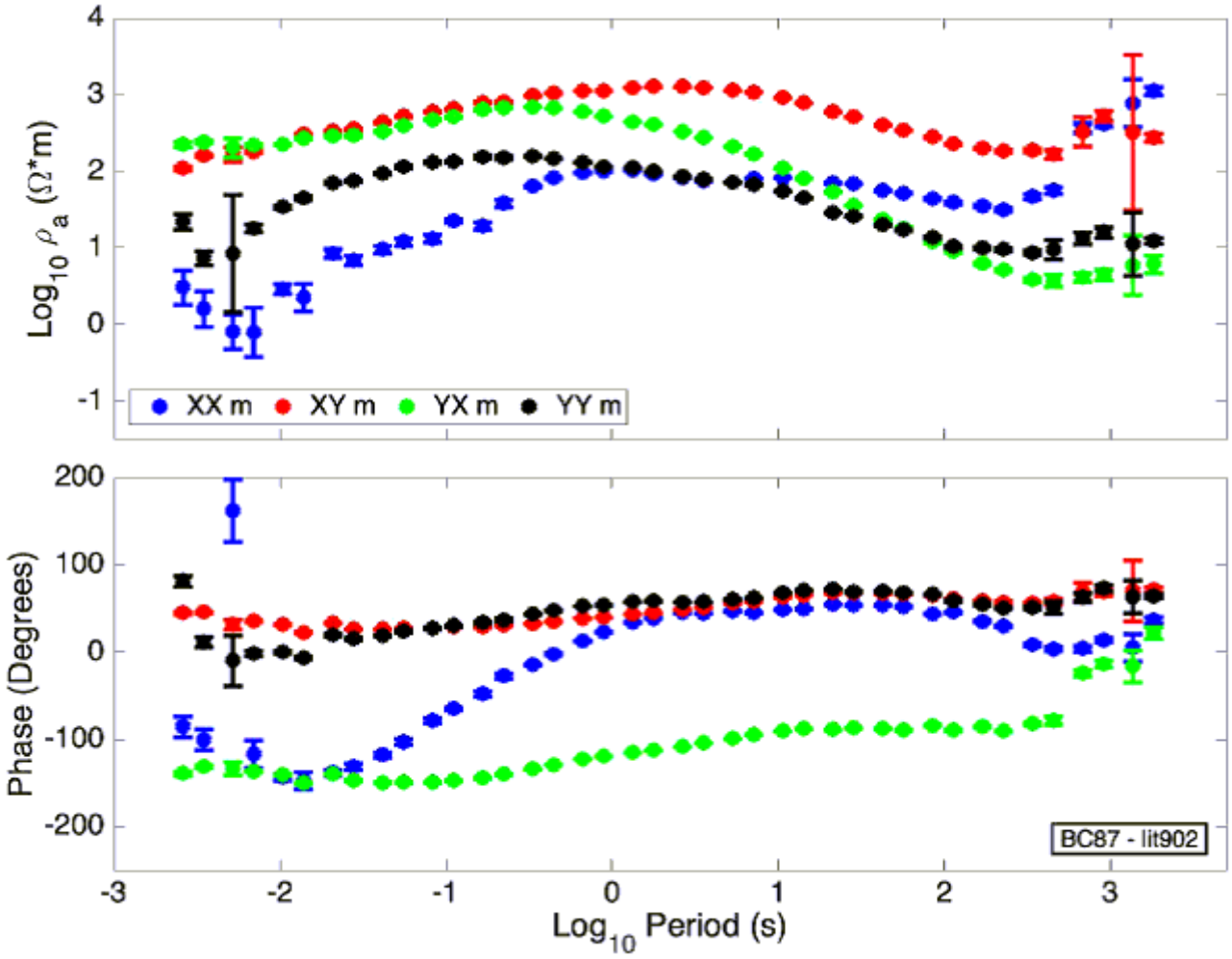

Figure 15

Data of site lit902 of the BC87 dataset.

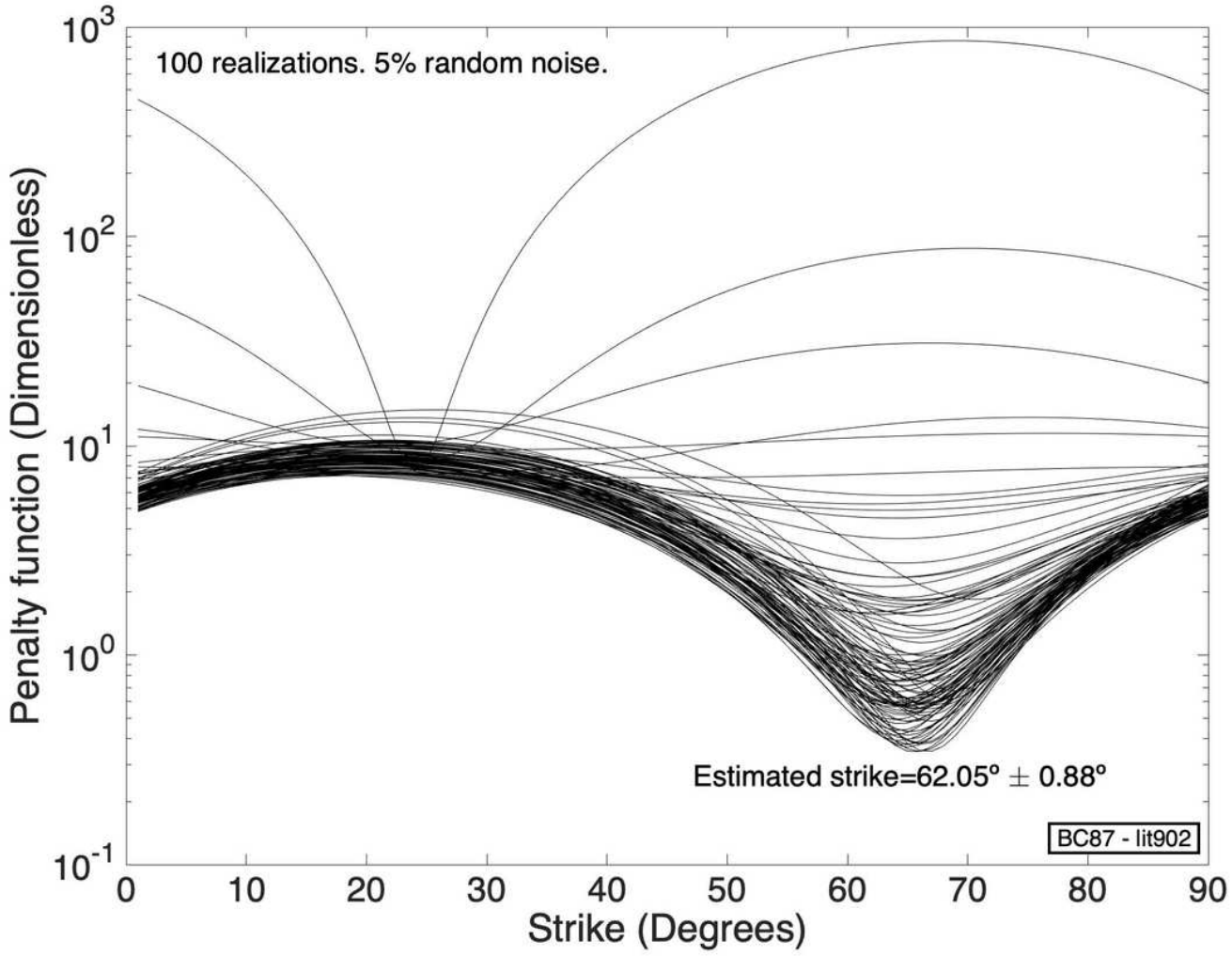

Figure 16

Estimation of strike using the reframed version of the phase tensor for a window that includes all the available periods.

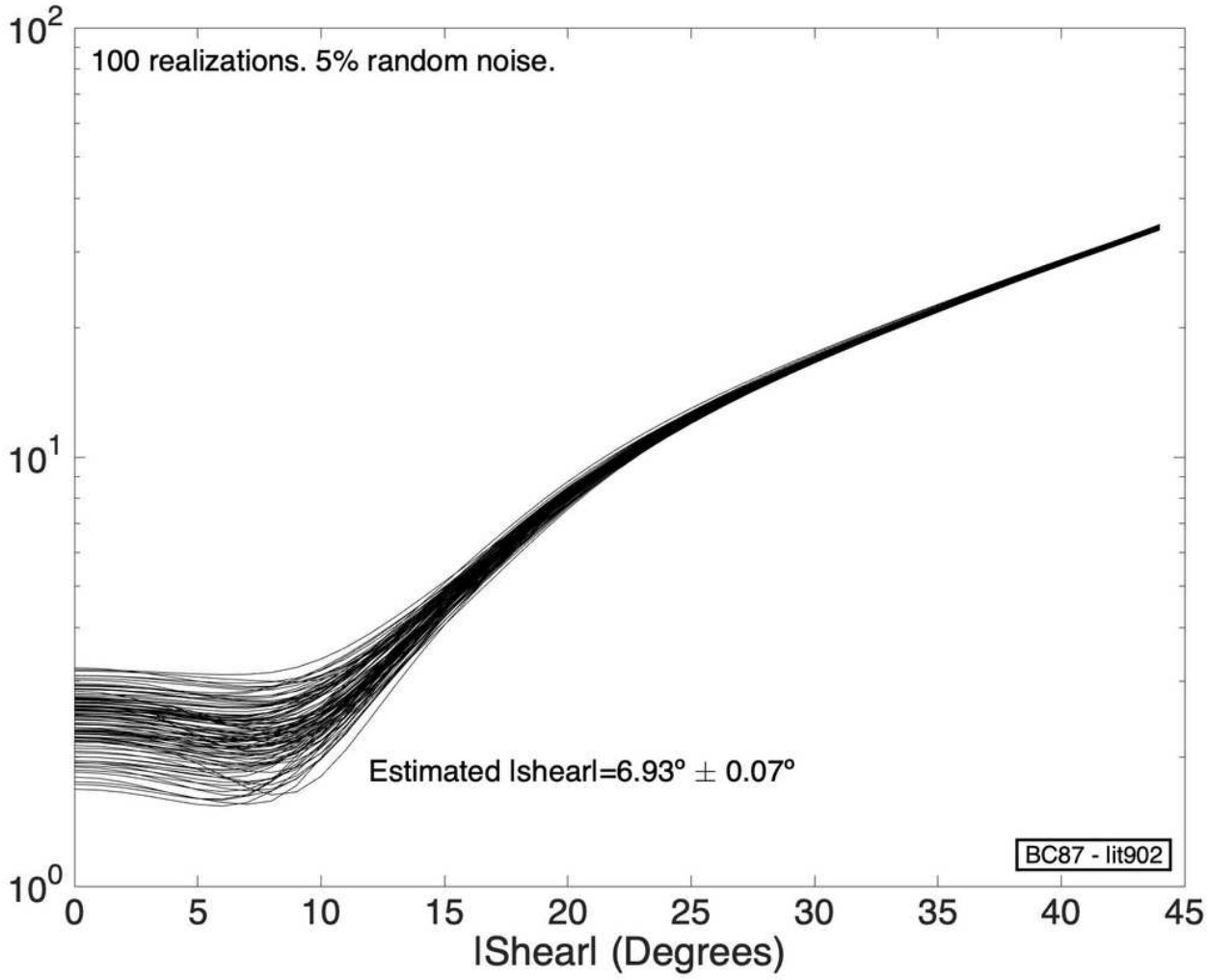

Figure 17

Estimation of the absolute value of shear comparing the phases from the quadratic equation and from the phase tensor. The optimum absolute value of shear is the average of the corresponding minima.

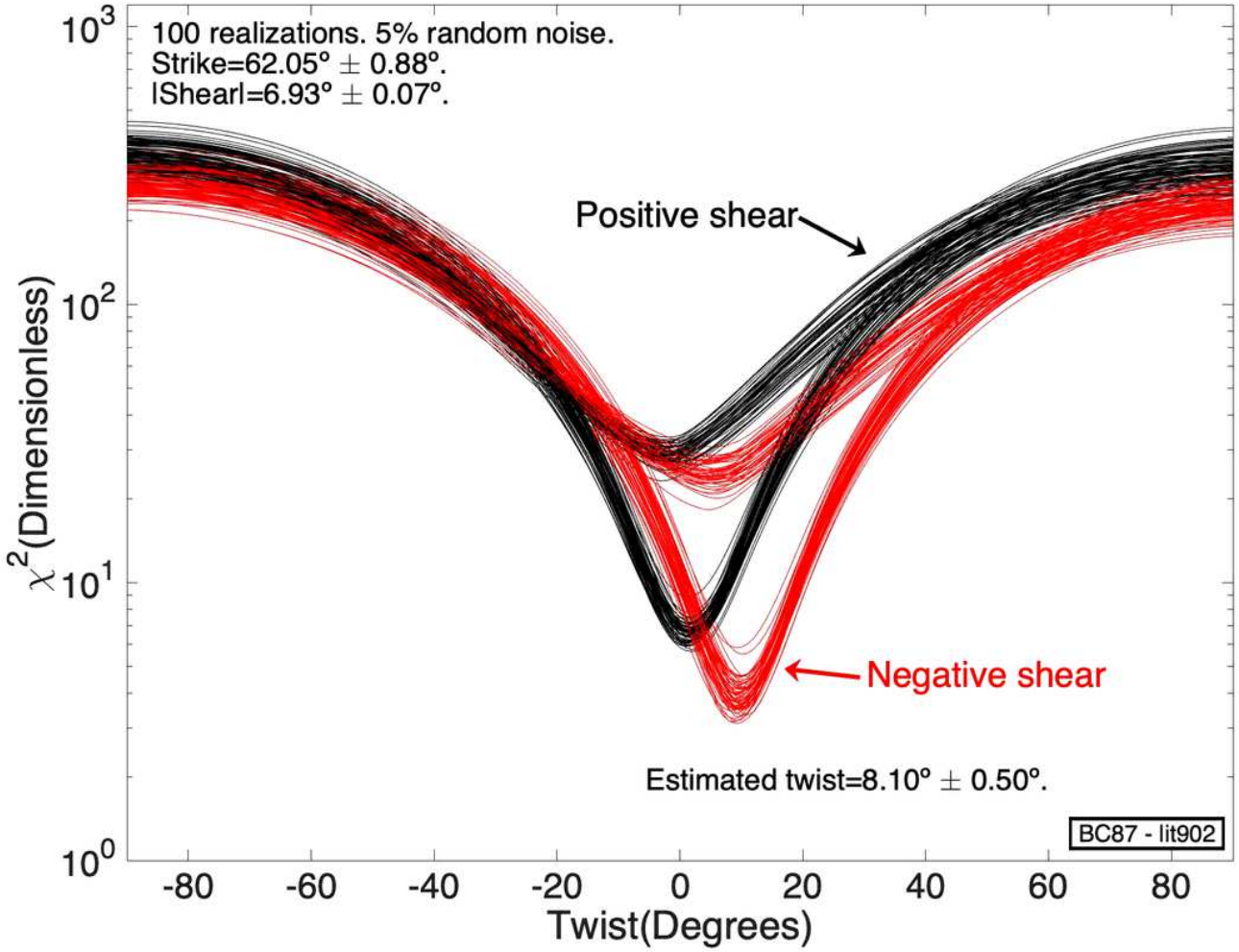

Figure 18

Site lit902 of the BC87 dataset. χ^2 objective functions for the estimation of twist assuming the two possibilities for the unknown sign of shear.

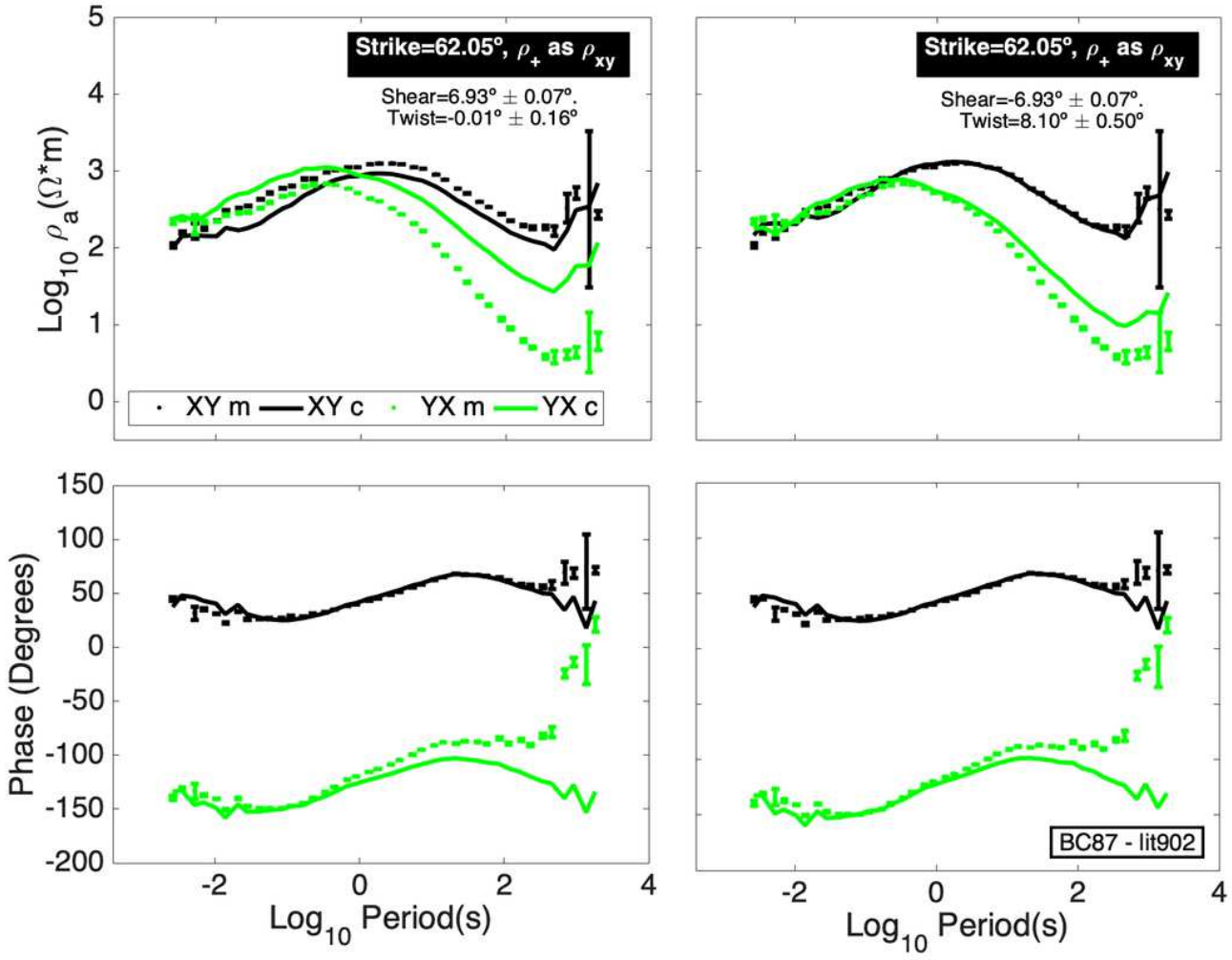

Figure 19

Site lit902 of the BC87 dataset. Comparison of the data with the response of the distortion model assuming positive and negative shears.

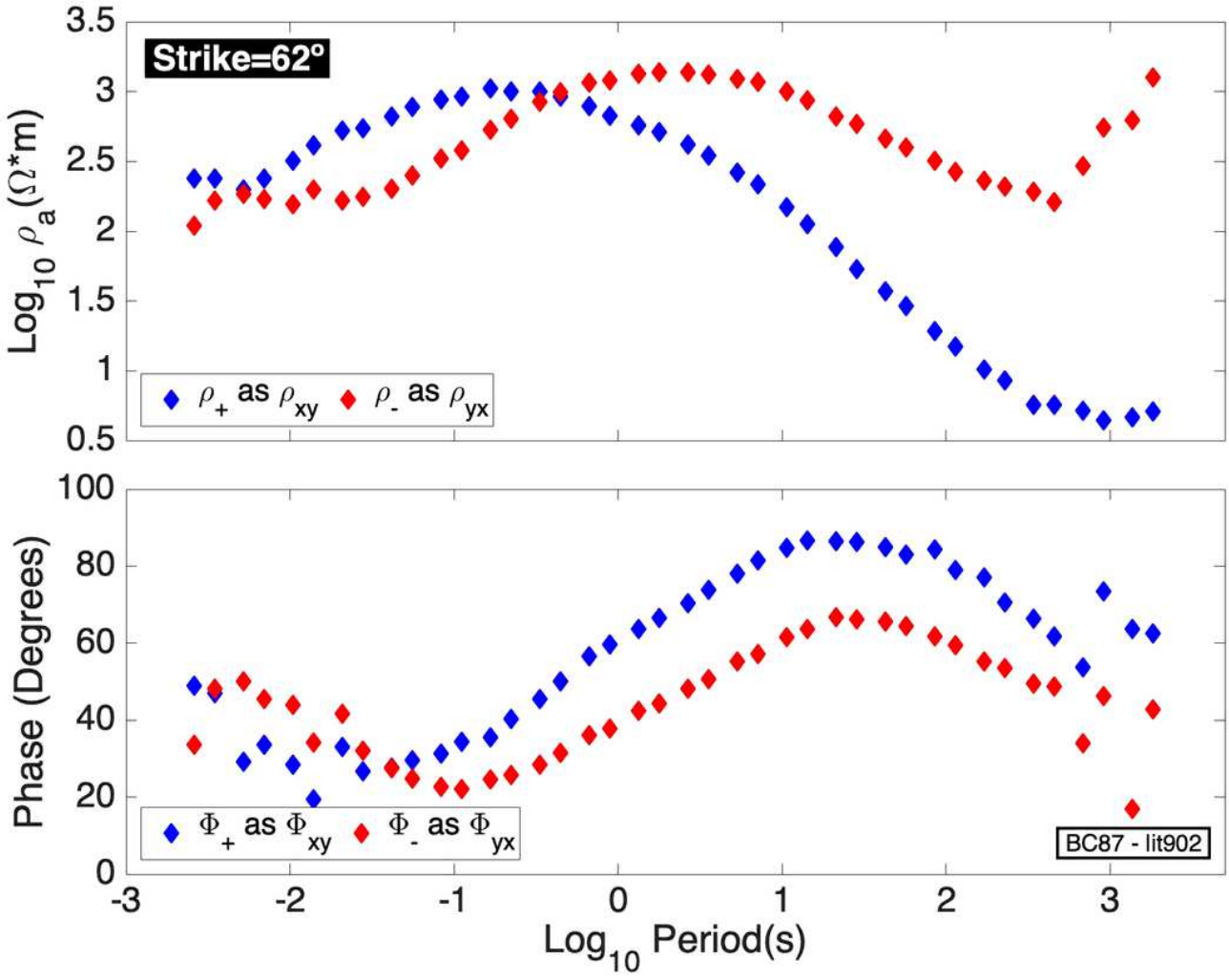

Figure 20

These graphs summarize the output of the process of linking strike angles to invariant impedances. The graphical abstract at the beginning of the article considers the classical ambiguity of 90 degrees.

Supplementary Files

This is a list of supplementary files associated with this preprint. Click to download.

- abstract.jpg